
High-probability complexity guarantees for nonconvex minimax problems

Yassine Laguel[†]

Laboratoire Jean Alexandre Dieudonné
Université Côte d’Azur, Nice, France
yassine.laguel@univ-cotedazur.fr

Yasa Syed[‡]

Department of Statistics, Rutgers University
Piscataway, New Jersey, USA
yasa.syed@rutgers.edu

Necdet Serhat Aybat[†]

Department of Industrial Engineering
Penn State University,
University Park, PA, USA.
nsa10@psu.edu

Mert Gürbüzbalaban^{‡*}

Department of Statistics, Rutgers University
Rutgers Business School, Rutgers University
Piscataway, New Jersey, USA
mg1366@rutgers.edu

Abstract

Stochastic smooth nonconvex minimax problems are prevalent in machine learning, e.g., GAN training, fair classification, and distributionally robust learning. Stochastic gradient descent ascent (GDA)-type methods are popular in practice due to their simplicity and single-loop nature. However, there is a significant gap between the theory and practice regarding high-probability complexity guarantees for these methods on stochastic nonconvex minimax problems. Existing high-probability bounds for GDA-type single-loop methods only apply to convex/concave minimax problems and to particular non-monotone variational inequality problems under some restrictive assumptions. In this work, we address this gap by providing the first high-probability complexity guarantees for nonconvex/PL minimax problems corresponding to a smooth function that satisfies the PL-condition in the dual variable. Specifically, we show that when the stochastic gradients are light-tailed, the smoothed alternating GDA method can compute an ε -stationary point within $\mathcal{O}(\frac{\ell\kappa^2\delta^2}{\varepsilon^4} + \frac{\kappa}{\varepsilon^2}(\ell + \delta^2 \log(1/\bar{q})))$ stochastic gradient calls with probability at least $1 - \bar{q}$ for any $\bar{q} \in (0, 1)$, where μ is the PL constant, ℓ is the Lipschitz constant of the gradient, $\kappa = \ell/\mu$ is the condition number, and δ^2 denotes a bound on the variance of stochastic gradients. We also present numerical results on a nonconvex/PL problem with synthetic data and on distributionally robust optimization problems with real data, illustrating our theoretical findings.

1 Introduction

Minimax optimization problems arise frequently in machine learning (ML) applications; indeed, constrained optimization problems such as deep learning with model constraints [24], dictionary learning [10, 53] or matrix completion [27] can be recast as a minimax optimization problem through Lagrangian duality. Other applications include but are not limited to the training of GANs [55], fair learning [69], supervised learning [57, 46, 48, 71], adversarial deep learning [72], game theory [50, 54], robust optimization [4, 3], distributionally robust learning [43, 72, 24], meta-learning [67] and multi-agent reinforcement learning [15]. Many of these applications can be reformulated in the following minimax form:

$$\min_{x \in \mathbb{R}^{d_1}} \max_{y \in \mathbb{R}^{d_2}} f(x, y), \quad (1)$$

*Corresponding author.

where $f : \mathbb{R}^{d_1} \times \mathbb{R}^{d_2} \rightarrow \mathbb{R}$ is a smooth function, i.e., differentiable with a Lipschitz gradient; f can possibly be nonconvex in x and nonconcave in y . First-order primal-dual (FOPD) methods have been the leading computational approach for computing low-to-medium-accuracy stationary points for these problems because of their cheap iterations and mild dependence of their overall complexities on the problem dimension and data size [9, 8, 35]. In the context of FOPD methods, there are two key settings for (1):

- (i) the *deterministic* setting, where the partial gradients $\nabla_x f$ and $\nabla_y f$ are exactly available,
- (ii) the *stochastic* setting, where we have only access to (inexact) stochastic estimates of the partial gradients, in which case the problem in (1) is called a *stochastic minimax problem*.

It can be argued that the stochastic setting is more relevant to modern machine learning applications where gradients are typically estimated randomly from mini-batches of data, or sometimes intentionally perturbed with random noise to ensure data privacy [14, 33, 1].

Convex and nonconvex minimax optimization. In the convex case (when f is convex² in x and concave in y), several approaches have been considered including Variational Inequalities (VIs) and primal-dual algorithms, see. e.g. [28, 20, 5, 64, 12, 70, 56, 11] and the references therein. One disadvantage of using the VI approach for solving minimax problems (by identifying the *signed gradient map* $G(x, y) \triangleq [\nabla_x f(x, y)^\top, -\nabla_y f(x, y)^\top]^\top$ as the corresponding operator in the VI) is that one needs to set the primal and dual stepsize to be the same. This can be restrictive in applications where f exhibits different smoothness properties in the primal (x) and dual (y) block coordinates –this is often the case in distributionally robust learning [70], adversarial learning [41] and in the Lagrangian reformulations of constrained optimization problems that involve many constraints [44]. The gap function $\mathcal{G}(x_k, y_k) \triangleq \sup_{x, y} f(x_k, y) - f(x, y_k)$, and the squared distance to the set of saddle points $\mathcal{D}(x_k, y_k) \triangleq \min\{\|x_k - x^*\|^2 + \|y_k - y^*\|^2 \mid (x^*, y^*) \text{ is a saddle point}\}$ are standard metrics for assessing the quality of the output $z_k = (x_k, y_k)$ generated by an FOPD algorithm after k iterations among many others [34, 70, 20].

In the nonconvex setting, i.e., when f is nonconvex in x , the aim is to compute a stationary point. Let $\mathcal{M}(x_k, y_k)$ denote a measure for the *stationarity* of iterates (x_k, y_k) ; a common metric is the norm of the gradient, i.e., $\mathcal{M}(x_k, y_k) \triangleq \|\nabla f(x_k, y_k)\|$ and its variants such as $\|\nabla \Phi(x_k)\|$ when f is strongly concave in y , where $\Phi(\cdot) = \max_y f(\cdot, y)$ denotes the primal function –for other metrics and relation between them, see [58]. There are several algorithms that admit (gradient) complexity guarantees for computing a stationary point of nonconvex minimax problems under various strong concavity, concavity or weak concavity-type assumptions in the y variable –see the references in [58].

In expectation and high-probability bounds. Most of the existing guarantees in the literature for *stochastic* FOPD algorithms are provided in expectation, i.e., a bound on the number of iterations k (or the stochastic gradient evaluations) is provided for $\mathbb{E}[\mathcal{G}(x_k, y_k)] \leq \varepsilon$ or $\mathbb{E}[\mathcal{D}(x_k, y_k)] \leq \varepsilon$ to hold (see, e.g., [70, 69, 28] and the references therein). While high-probability guarantees have been considered in the literature [34, 36, 60, 20, 31, 22], they mostly apply to the monotone VI setting, or to strongly convex/strongly concave (SCSC) minimax problems. To our knowledge, existing guarantees in the nonconvex setting only hold in expectation, i.e., providing bounds on $\mathbb{E}[\mathcal{M}(x_k, y_k)]$. The issue is that having such guarantees *on average* does not allow us to control tail events, i.e., even if $\mathbb{E}[\mathcal{M}(x_k, y_k)]$ is small, $\mathcal{M}(x_k, y_k)$ can still be arbitrarily large with a non-zero probability. Therefore, high-probability results are needed for controlling the risk associated with the worst-case tail events because they specify how many iterations are necessary to ensure $\mathcal{M}(x_k, y_k)$ is sufficiently small for any given failure probability $\bar{q} \in (0, 1)$. Yet, high-probability guarantees for nonconvex minimax problems are non-existent in the literature, even for nonconvex/strongly concave (NCSC) problems. In fact, the existing VI literature with high-probability bounds on non-monotone operators such as star-co-coercive operators [20, 51], do not apply to NCSC problems.³

New high-probability bounds for NCPL optimization. To address these shortcomings, we focus on developing high-probability guarantees for NCPL problems, where f is a smooth function such that it is possibly nonconvex in x and it satisfies a Polyak-Lojasiewicz (PL) condition in y . The

² $\hat{f} : \mathbb{R}^d \rightarrow \mathbb{R} \cup \{+\infty\}$ is called (merely) convex, if $\hat{f}(tx_1(1-t)x_2) \leq t\hat{f}(x_1) + (1-t)\hat{f}(x_2)$ for every $x_1, x_2 \in \mathbb{R}^d$ and $t \in [0, 1]$ with the convention that $\alpha \leq +\infty$ for all $\alpha \in \mathbb{R}$.

³ For example, when ∇f is smooth (Lipschitz and continuously differentiable) and the signed gradient map $G(x, y)$ is star-cocoercive with constant $\ell > 0$ around a stationary point (x_*, y_*) , then by [21, Lemma C.6], the operator $\text{Id} - \frac{2}{\ell}G(x, y)$ is non-expansive around (x_*, y_*) ; thus, the Jacobian of G at (x_*, y_*) has non-negative eigenvalues implying f is merely convex/merely concave around (x_*, y_*) , i.e., f cannot be NCSC.

PL condition is a weaker assumption (milder condition) than strong concavity in y ; therefore, our results will also hold for the class of NCSC problems –in fact, PL condition in the dual does not even require quasi-concavity. NCPL problems constitute a rich class of problems arising in many ML applications including but not limited to fair classification [45], robust neural network training with dual regularization [45, eqn. (14)], overparametrized systems and neural networks [40], linear quadratic regulators [17], smoothed Lasso problems [23] subject to constraints, distributionally robust learning with ℓ_2 regularization in the dual [69], deep AUC maximization [65] and covariance matrix learning with Wasserstein GANs [49].

Among the existing algorithms in the NCPL setting [60], stochastic gradient descent ascent (SGDA) methods and their variants are quite popular for ML applications, e.g., training GANs and adversarial learning, as SGDA is easy to implement due to its single-loop structure. Guarantees in expectation for stochastic NCSC problems are well supported by the literature [69, 59, 38, 6, 30, 29, 42, 62, 32] and the references therein. To our knowledge, among single-loop methods for NCPL problems, the best guarantees in expectation are given by the *smoothed* alternating gradient descent ascent (sm-AGDA) method [62], which can compute an almost stationary point (\tilde{x}, \tilde{y}) satisfying $\mathbb{E}[\|\nabla f(\tilde{x}, \tilde{y})\|] \leq \varepsilon$ in $\mathcal{O}(\ell\kappa^2\delta^2/\varepsilon^4 + \ell\kappa/\varepsilon^2)$ stochastic gradient calls, where $\mu > 0$ is the PL constant, ℓ denotes the Lipschitz constant for ∇f , δ^2 is an upper bound on the variance of the stochastic gradients, and $\kappa \triangleq \ell/\mu \geq 1$ is the condition number. In this work, we consider the sm-AGDA algorithm, and to our knowledge we provide the first-time high-probability bounds (using a single-loop method that does not resort to restarts and parallel runs) for the minimax problem (1) in the NCSC and NCPL settings. More precisely, we focus on a purely stochastic regime in which data streams over time which renders the use of mini-batch schemes or running the method in parallel impractical; therefore, approaches based on Markov’s inequality [58] are no longer applicable.

Contributions. Our contributions are threefold:

- We present the first *high-probability* complexity result for the sm-AGDA algorithm in the NCPL setting by building upon a Lyapunov function first introduced in [67] for nonconvex-concave problems. Later, for the same Lyapunov function, state-of-the-art complexity bounds in *expectation* are provided for the NCPL setting in [63]. In this paper, we derive a novel descent property for this Lyapunov function in the almost sure sense (Theorem 7 and Corollary 8), allowing us to develop useful concentration arguments for it to derive high-probability bounds. Our Lyapunov analysis not only sheds light on the convergence properties of sm-AGDA, but also guides the parameter selection for sm-AGDA. Specifically, we show that sm-AGDA can compute an almost stationary point (\tilde{x}, \tilde{y}) satisfying $\|\nabla f(\tilde{x}, \tilde{y})\| \leq \varepsilon$ with probability $1 - \bar{q} \in (0, 1)$ within $T_{\varepsilon, \bar{q}} = \mathcal{O}\left(\frac{\ell\kappa^2\delta^2}{\varepsilon^4} + \frac{\kappa}{\varepsilon^2}(\ell + \delta^2 \log(1/\bar{q}))\right)$ stochastic gradient calls. The lower complexity bound of $\Omega(\frac{1}{\varepsilon^2} + \frac{1}{\varepsilon^4})$ for NCSC problems [37, 68] in expectation (see also [59, 69]) suggests that our high-probability bound for sm-AGDA is tight in terms of its dependence on ε . Furthermore, to our knowledge, these are the first high-probability guarantees for any algorithm in the NCPL setting.
- Under light-tail (sub-Gaussian) assumption on the gradient noise (Assumption 3), which is common in the literature [34, 31, 19], we develop a new concentration result (Theorem 9) that can be of independent interest. From this concentration inequality, we observe that the cost of strengthening the existing complexity result in expectation to a high-probability one is relatively low, i.e., in the final complexity, the probability parameter \bar{q} *only* appears in an additive term that scales with ε^{-2} . Consequently, this represents a non-dominant overhead compared to the ε^{-4} term already present in state-of-the-art expectation bounds [63].
- Third, we provide experiments that illustrate our theoretical results. We first provide an example of an NCPL-game with synthetic data and then focus on distributionally robust optimization problems with real data, illustrating the performance of the sm-AGDA in terms of high-probability guarantees.

2 Preliminaries and Technical Background

Stationarity metric. We consider the minimax problem in (1) for $f : \mathbb{R}^{d_1} \times \mathbb{R}^{d_2} \rightarrow \mathbb{R}$ such that f is smooth (Assumption 1) and $f(x, \cdot)$ satisfies the PL property for all $x \in \mathbb{R}^{d_1}$ (Assumption 2); moreover, we also assume that we only have access to unbiased stochastic estimates of ∇f such that the stochastic error $G(x, y, \xi) - \nabla f(x, y)$ has a light tail (Assumption 3) for any (x, y) , where $G(x, y, \xi)$ denote the stochastic estimate of $\nabla f(x, y)$ and ξ denotes the randomness in the estimator.

Algorithm	Complexity	Problem	Metric	NC?
Epoch-GDA [60] [†]	$\mathcal{O}\left(\frac{\delta^2}{\mu_s \varepsilon} \log(1/\bar{q})\right)$	SCSC	$\mathcal{G}(\bar{z}_k)$	✗
Clipped-SGDA [20] [‡]	$\tilde{\mathcal{O}}\left(\max\left\{\frac{\ell}{\mu_s}, \frac{\delta^2}{\mu_s \varepsilon}\right\} \log\left(\frac{1}{\varepsilon}\right) \log(\kappa/\bar{q})\right)$	SCSC	$\mathcal{D}(z_k)$	✗
Clipped-SEG [20] [§]	$\tilde{\mathcal{O}}\left(\max\left\{\frac{\ell}{\mu_s}, \frac{\delta^2}{\mu_s \varepsilon}\right\} \log\left(\frac{1}{\varepsilon}\right) \log(\kappa/\bar{q})\right)$	SCSC	$\mathcal{D}(z_k)$	✗
Stochastic APD [34] ^{▷*}	$\mathcal{O}\left(\frac{\ell \log\left(\frac{1}{\varepsilon}\right)}{\mu_s} + \frac{(1+\log(1/\bar{q}))\delta^2 \log(1/\varepsilon)}{\mu_s \varepsilon}\right)$	SCSC	$\mathcal{D}(z_k)$	✗
Mirror-Prox [31] [*]	$\mathcal{O}\left(\max\left(\frac{\ell D^2}{\varepsilon^2}, \frac{\sigma^2 D^2}{\varepsilon^2}\right) \log(1/\bar{q})\right)$	MCMC	$\mathcal{G}(\bar{z}_k)$	✗
Clipped-SGDA [20] [‡]	$\tilde{\mathcal{O}}\left(\max\left\{\frac{1}{\varepsilon}, \frac{\delta^2 R^2}{\varepsilon^2}\right\} \log(1/\bar{q})\right)$	MCMC	$\mathcal{G}_R(\bar{z}_k)$	✗
Clipped-SEG [20]	$\tilde{\mathcal{O}}\left(\max\left(\frac{\ell R^2}{\varepsilon}, \frac{\sigma^2 R^2}{\varepsilon^2}\right) \log(1/\bar{q})\right)$	MCMC	$\mathcal{G}_R(\bar{z}_k)$	✗
sm-AGDA [Our Paper, Coro. 12] [*]	$\mathcal{O}\left(\frac{\ell \kappa^2 \delta^2}{\varepsilon^4} + \frac{\kappa}{\varepsilon^2} (\ell + \delta^2 \log(1/\bar{q}))\right)$	NCPL	$\frac{1}{k+1} \sum_{j=0}^k \ \nabla f(z_j)\ ^2$	✓

Table 1: Summary of the high-probability bounds for minimax problem classes when the gradient of f is Lipschitz (with parameter ℓ) and stochastic gradient variance is bounded by δ^2 . The second column reports the complexity (number of calls to stochastic gradient oracle) required to achieve the (stationarity) metric reported in the fourth column to be at most ε with probability $1 - \bar{q} \in (0, 1)$; $\tilde{\mathcal{O}}(\cdot)$ ignores some logarithmic terms. Here, μ_s is the strong convexity constant, μ is the PL constant, and $\kappa \triangleq \ell/\mu$. Let $G(z) \triangleq [\nabla_x f(z)^\top, -\nabla_y f(z)^\top]^\top$ with $z = (x, y)$ and $\bar{z}_k = \frac{1}{K+1} \sum_{j=0}^K z_j$, $\mathcal{G}(z) \triangleq \max_{\{\bar{z} \in Z\}} \langle G(z), \bar{z} - z_* \rangle$, where Z is the domain of the problem with diameter $D \in (0, +\infty]$, and $\mathcal{G}_R(z) \triangleq \max_{\{\bar{z} \in Z: \|\bar{z} - z_*\| \leq R\}} \langle G(z), \bar{z} - z_* \rangle$ where $z_* = (x_*, y_*^\top)^\top$ is a stationary point. The third column reports the minimax problem class. The fifth column indicates whether the results supports nonconvexity, i.e., whether f can be a smooth function nonconvex in x . [†] [60] is a two-loop method. [‡] Applicable to quasi-strongly monotone G that is star-co-coercive around z_* and supports heavy-tailed gradients. [§] Applicable to quasi-strongly monotone G and supports heavy-tailed gradients. [▷] Supports proximal steps to handle non-smooth convex penalty. ^{*} Applies to monotone G that is star-co-coercive around z_* . ^{*} Makes a light-tail assumption (Ass. 3).

Our aim is to compute a $(\varepsilon_x, \varepsilon_y)$ -stationary point (\tilde{x}, \tilde{y}) for (1) such that $\|\nabla_x f(\tilde{x}, \tilde{y})\| \leq \varepsilon_x$ and $\|\nabla_y f(\tilde{x}, \tilde{y})\| \leq \varepsilon_y$. We also call (\tilde{x}, \tilde{y}) an ε -stationary point if $\|\nabla f(\tilde{x}, \tilde{y})\| \leq \varepsilon$. Clearly, whenever (\tilde{x}, \tilde{y}) is $(\varepsilon_x, \varepsilon_y)$ -stationary, then it is also ε -stationary for $\varepsilon = (\varepsilon_x^2 + \varepsilon_y^2)^{1/2}$.

Smoothed alternating gradient descent ascent (sm-AGDA): The method can be considered as an *inexact* proximal point method and was introduced in [67]. More specifically, in each iteration of sm-AGDA, given a proximal center z_t and the current iterate (x_t, y_t) , the method computes the next iterate (x_{t+1}, y_{t+1}) using a stochastic gradient descent ascent step on a regularized function \hat{f} :

$$\hat{f}(x, y; z_t) \triangleq f(x, y) + \frac{p}{2} \|x - z_t\|^2. \quad (2)$$

Following the stochastic alternating gradient descent ascent (stochastic AGDA) steps, the *proximal center* at iteration t , i.e., z_t , is updated as shown in Algorithm 1, where $G_x(x_t, y_t, \xi_{t+1}^x)$ and $G_y(x_{t+1}, y_t, \xi_{t+1}^y)$ denote conditionally unbiased stochastic estimators of the gradients $\nabla_x f(x_t, y_t)$ and $\nabla_y f(x_{t+1}, y_t)$. Throughout the analysis we assume that ∇f is Lipschitz, which is standard in the study of first-order optimization algorithms for smooth minimax problems; see, e.g., [69, 70, 72, 59].

Assumption 1. (Lipschitz gradient) For all $(x_1, y_1), (x_2, y_2) \in \mathbb{R}^{d_1} \times \mathbb{R}^{d_2}$, there exists $\ell > 0$

$$\|\nabla_x f(x_1, y_1) - \nabla_x f(x_2, y_2)\| \leq \ell(\|x_1 - x_2\| + \|y_1 - y_2\|) \quad (3)$$

$$\|\nabla_y f(x_1, y_1) - \nabla_y f(x_2, y_2)\| \leq \ell(\|x_1 - x_2\| + \|y_1 - y_2\|). \quad (4)$$

The following condition, known as Polyak-Łojasiewicz (PL) condition is weaker than assuming strong concavity in y , and does not even necessitate f to be even quasi-concave in the y variable. It holds in many ML applications including those in [45, 45, 40, 17, 23, 69, 65, 49, 63].

Assumption 2. (PL condition in y) For every $x \in \mathbb{R}^{d_1}$, $\max_{y \in \mathbb{R}^{d_2}} f(x, y)$ has a non-empty solution set and a finite optimal value. Moreover, there exists $\mu > 0$ such that:

$$\|\nabla_y f(x, y)\|^2 \geq 2\mu [\max_{y \in \mathbb{R}^{d_2}} f(x, y) - f(x, y)], \quad \forall x \in \mathbb{R}^{d_1}. \quad (5)$$

We assume that we have only access to stochastic estimates $G_x(x_t, y_t, \xi_{t+1}^x)$ and $G_y(x_{t+1}, y_t, \xi_{t+1}^y)$ of the partial gradients $\nabla_y f(x_k, y_k)$ and $\nabla_x f(x_{t+1}, y_t)$, where ξ_{t+1}^x and ξ_{t+1}^y are random variables defined on a probability space (Ω, \mathbb{P}) , i.e., the source of randomness in the gradient estimates. Note that sm-AGDA has Gauss-Seidel updates, i.e., the stochastic estimate of the partial gradient $G_y(x_{t+1}, y_t, \xi_{t+1}^y)$ is evaluated at the updated point (x_{t+1}, y_t) instead of (x_t, y_t) . To capture

Algorithm 1 sm-AGDA

Input: $(x_0, y_0, z_0), \tau_1, \tau_2 > 0, \beta \in [0, 1], p \geq 0$

for $t = 0, 1, 2, \dots, T-1$ **do**

$$x_{t+1} = x_t - \tau_1 [G_x(x_t, y_t, \xi_{t+1}^x) + p(x_t - z_t)]$$

$$y_{t+1} = y_t + \tau_2 G_y(x_{t+1}, y_t, \xi_{t+1}^y)$$

$$z_{t+1} = z_t + \beta(x_{t+1} - z_t)$$

end for

Output: choose (\tilde{x}, \tilde{y}) uniformly from $\{(x_t, y_t)\}_{t=0}^{T-1}$

the sequential information flow, we next introduce the natural filtrations that represent all the information available before an update: Let ξ_t^x and ξ_t^y be revealed sequentially in the natural order of the sm-AGDA updates, i.e., $\xi_1^x \rightarrow \xi_1^y \rightarrow \xi_2^x \rightarrow \xi_2^y \rightarrow \xi_3^x \rightarrow \dots$, and let $(\mathcal{F}_t^x)_{t \geq 1}$ and $(\mathcal{F}_t^y)_{t \geq 1}$ denote the associated filtration⁴, i.e., let $\mathcal{F}_0^y \triangleq \{\emptyset, \Omega\}$, and

$$\mathcal{F}_{t+1}^x = \sigma(\mathcal{F}_t^y, \sigma(\xi_{t+1}^x)), \quad \mathcal{F}_{t+1}^y = \sigma(\mathcal{F}_{t+1}^x, \sigma(\xi_{t+1}^y)), \quad \forall t \geq 0. \quad (6)$$

Introducing multiple filtrations to represent the sequential information flow is common in the study of stochastic algorithms with Gauss-Seidel updates –see, e.g., papers on stochastic ADMM, and [7, 66]; and we follow the same approach. Consider the gradient noise (errors) at time $t \in \mathbb{N}$:

$$\Delta_t^x \triangleq G_x(x_t, y_t, \xi_{t+1}^x) - \nabla_x f(x_t, y_t), \quad \Delta_t^y \triangleq G_y(x_{t+1}, y_t, \xi_{t+1}^y) - \nabla_y f(x_{t+1}, y_t).$$

Finally, we also assume that the gradient noise is unbiased conditionally on the past information and that it admits a light (sub-Gaussian) tail.

Assumption 3. (Light tail) For any $t \geq 0$, there exists scalars $\delta_x, \delta_y > 0$ such that

$$\mathbb{E} [\Delta_t^x | \mathcal{F}_t^y] = 0, \quad \mathbb{P} [\|\Delta_t^x\| \geq s | \mathcal{F}_t^y] \leq 2e^{\frac{-s^2}{2\delta_x^2}}, \quad (7)$$

$$\mathbb{E} [\Delta_t^y | \mathcal{F}_{t+1}^x] = 0, \quad \mathbb{P} [\|\Delta_t^y\| \geq s | \mathcal{F}_{t+1}^x] \leq 2e^{\frac{-s^2}{2\delta_y^2}}. \quad (8)$$

For developing high-probability bounds in the learning context, it is common to assume that gradient estimates are sub-Gaussian [31, 34, 18]. While this assumption may not always hold (see e.g. [25, 52]), it often holds when gradients are estimated via mini-batching, as a consequence of the central limit theorem. It will also hold when the gradient noise is bounded. Additionally, adoption of differential privacy mechanisms within gradient-based schemes [14, 33, 1], to enhance data privacy, results frequently in sub-Gaussian gradient errors.

3 High-probability bounds for sm-AGDA

For analyzing sm-AGDA, similar to [62, 67], we consider the following Lyapunov function:

$$V_t \triangleq V(x_t, y_t; z_t) = \hat{f}(x_t, y_t; z_t) + 2P(z_t) - 2\Psi(y_t; z_t), \quad (9)$$

where $P(z)$ and $\Psi(\cdot; z)$ denote the saddle point value and the dual function value, respectively, of the auxiliary problem $\min_x \max_y \hat{f}(x, y; z)$ for any fixed z and \hat{f} defined in (2), i.e.,

$$\Psi(y; z) \triangleq \min_{x \in \mathbb{R}^{d_1}} \hat{f}(x, y; z) \quad \text{and} \quad P(z) \triangleq \min_{x \in \mathbb{R}^{d_1}} \max_{y \in \mathbb{R}^{d_2}} \hat{f}(x, y; z). \quad (10)$$

Next, we introduce a natural assumption, commonly made in the literature [63, 61]. Without this assumption, there are pathological cases where primal function $\Phi(x)$ may be unbounded leading to divergence of gradient-based methods; an example would be $f(x, y) = -x^2 - y^2$ in dimension one.

Assumption 4. Consider the primal function $\Phi : \mathbb{R}^{d_1} \rightarrow \mathbb{R}$, i.e., $\Phi(x) = \max_{y \in \mathbb{R}^{d_2}} f(x, y)$. There exists $x^* \in \mathbb{R}^{d_1}$ such that $\Phi^* \triangleq \Phi(x^*) = \min_{x \in \mathbb{R}^{d_1}} \Phi(x)$.

Under Assumption 4, it immediately follows that $V_t \geq \Phi^*$ for all $t \in \mathbb{N}$ –since $P(z) - \Psi(y, z) \geq 0$, $\hat{f}(x, y; z) - \Psi(y; z) \geq 0$ and $P(z) \geq \Phi^*$ for all x, y, z . We will next study the change $V_t - V_{t+1}$ in the Lyapunov function and show that an approximate descent property holds. First, we need two key lemmas that characterize the evolution of $\hat{f}(x_t, y_t; z_t)$ and $\Psi(y_t; z_t)$ over the iterations.

Lemma 5. Suppose Assumptions 1, 2, 3 and 4 hold. Consider sm-AGDA given in Alg. 1 with $\tau_1 \in (0, \frac{1}{p+\ell}]$ and $\beta \in (0, 1]$. For any $t \in \mathbb{N}$, we have:

$$\begin{aligned} \hat{f}(x_{t+1}, y_{t+1}; z_{t+1}) - \hat{f}(x_t, y_t; z_t) &\leq -\frac{\tau_1}{2} \|\nabla_x \hat{f}(x_t, y_t; z_t)\|^2 + \tau_2 \left(1 + \frac{\ell}{2}\tau_2\right) \|\nabla_y f(x_{t+1}, y_t)\|^2 \\ &\quad + \tau_1((p + \ell)\tau_1 - 1) \langle \Delta_t^x, \nabla_x \hat{f}(x_t, y_t; z_t) \rangle + \frac{p + \ell}{2} \tau_1^2 \|\Delta_t^x\|^2 \\ &\quad + \tau_2(1 + \ell\tau_2) \langle \nabla_y f(x_{t+1}, y_t), \Delta_t^y \rangle - \frac{p}{2\beta} \|z_t - z_{t+1}\|^2 + \frac{\ell\tau_2^2}{2} \|\Delta_t^y\|^2. \end{aligned}$$

⁴Given a random variable ξ , $\sigma(\xi)$ denotes the σ -algebra generated by ξ ; moreover, given two σ -algebras, Σ_1 and Σ_2 , abusing the notation, $\sigma(\Sigma_1, \Sigma_2)$ denotes the σ -algebra generated by $\Sigma_1 \cup \Sigma_2$.

Proof. The proof is provided in Appendix B.1. \square

From Assumption 1, when $p > \ell$, the auxilliary function $\hat{f}(\cdot, y; z)$ is $(p - \ell)$ -strongly convex for any fixed y, z ; hence, there is a unique minimizer for every y, z fixed, denoted by

$$x^*(y, z) \triangleq \operatorname{argmin}_{x \in \mathbb{R}^{d_1}} \hat{f}(x, y; z), \quad (11)$$

i.e., $\Psi(y, z) = \hat{f}(x^*(y, z), y; z)$. In the rest of the paper, we will take $p > \ell$ and exploit this property. The following lemma characterizes the change in the dual function Ψ .

Lemma 6. *Suppose Assumptions 1, 2, 3 and 4 hold. Consider the sm-AGDA iterate sequence $\{(x_t, y_t, z_t)\}_{t \in \mathbb{N}}$ for $p > \ell$. For any $t \in \mathbb{N}$, it holds that*

$$\begin{aligned} \Psi(y_{t+1}; z_{t+1}) - \Psi(y_t; z_t) &\geq \tau_2 \langle \nabla_y f(x^*(y_t, z_t), y_t), \nabla_y f(x_{t+1}, y_t) \rangle + \tau_2 \langle \nabla_y f(x^*(y_t, z_t), y_t), \Delta_t^y \rangle \\ &\quad - \frac{L_\Psi}{2} \tau_2^2 (\|\nabla_y f(x_{t+1}, y_t)\|^2 + 2 \langle \nabla_y f(x_{t+1}, y_t), \Delta_t^y \rangle + \|\Delta_t^y\|^2) \\ &\quad + \frac{p}{2} \langle z_{t+1} - z_t, z_{t+1} + z_t - 2x^*(y_{t+1}, z_{t+1}) \rangle, \end{aligned}$$

where $L_\Psi \triangleq \ell \left(1 + \frac{p+\ell}{p-\ell}\right)$ and the map $x^*(\cdot, \cdot)$ is defined by (11).

Proof. The proof is provided in Appendix B.2. \square

The next result provides an approximate descent property on the Lyapunov function. Its proof builds on Lemmas 5 and 6 and a descent property on the function P (given in Lemma 13 of the Appendix); and leverages smoothness properties of the functions \hat{f} and Ψ and the map $(y, z) \mapsto x^*(y, z)$ as well as the strong convexity of \hat{f} with respect to x .

Theorem 7. *Suppose Assumptions 1, 2, 3 and 4 hold. Consider the sm-AGDA algorithm with parameters $p > \ell$, $\beta \in (0, 1]$, $\tau_1 \in (0, \frac{1}{p+\ell}]$ and $\tau_2 > 0$ chosen such that*

$$c_0 \triangleq -\tau_2^2 \ell \nu + \tau_2 \left(1 - \frac{\ell}{2} \tau_2 - L_\Psi \tau_2\right) \geq 0, \quad c'_0 \triangleq \frac{p}{3\beta} - \left(\frac{2p^2}{p-\ell} + 48\beta \frac{p^3}{(p-\ell)^2}\right) \geq 0,$$

for some constant $\nu > 0$, where $L_\Psi = \ell \left(1 + \frac{p+\ell}{p-\ell}\right)$. Then,

$$\begin{aligned} V_t - V_{t+1} &\geq c_1 \|\nabla_x \hat{f}(x_t, y_t; z_t)\|^2 + c_2 \|\nabla_y f(x^*(y_t, z_t), y_t)\|^2 + c_3 \|x_t - z_t\|^2 \\ &\quad + c_4 \langle \nabla_x \hat{f}(x_t, y_t; z_t), \Delta_t^x \rangle + \langle c_5 \nabla_y f(x_t, y_t) + c_6 \nabla_y f(x^*(y_t, z_t), y_t), \Delta_t^y \rangle \\ &\quad + c_7 \|\Delta_t^x\|^2 + c_8 \|\Delta_t^y\|^2, \end{aligned} \quad (12)$$

for some constants $\{c_i\}_{i=1}^8 \subset \mathbb{R}$ that are explicitly given in Appendix C, which may depend on ν , as well as the problem and sm-AGDA parameters that can be chosen such that $c_1, c_2, c_3 > 0$.

Proof. The proof is given in Appendix C. \square

With some specific choice of parameters in sm-AGDA, we can obtain simplifications to the coefficients $\{c_i\}_{i=1}^8$ from Theorem 7 (explicitly given in Appendix C). As such, this yields the following corollary.

Corollary 8. *Under the premise of Theorem 7, let $p = 2\ell$, $\tau_1 \in (0, \frac{1}{3\ell}]$, $\tau_2 = \frac{\tau_1}{48}$, $\beta = \alpha \mu \tau_2$ for $\alpha \in (0, \frac{1}{406}]$. Then, $\frac{\tilde{A}_{t+1} - \tilde{A}_t}{\tau_1} \leq -\tilde{B}_t + \tilde{C}_{t+1} + \tilde{D}_{t+1}$ for all $t \in \mathbb{N}$, where $\nu = \frac{12}{\tau_1 \ell}$ and*

$$\begin{aligned} \tilde{A}_t &\triangleq \tau_1 V_t, \quad \tilde{B}_t \triangleq \frac{\tau_1}{5} \|\nabla_x \hat{f}(x_t, y_t; z_t)\|^2 + \frac{\tau_2}{8} \|\nabla_y f(x^*(y_t, z_t), y_t)\|^2 + \frac{\beta p}{8} \|x_t - z_t\|^2, \\ \tilde{C}_{t+1} &\triangleq \left[\left(192\beta p \left(\frac{p+\ell}{p-\ell} \right)^2 \ell^2 \tau_2^2 + \frac{4\ell}{\nu} + 4c_0 \ell^2 + 2c'_0 \beta^2 \right) \tau_1^2 + \left((p+\ell) \tau_1 - 1 \right) \tau_1 \right] \langle \nabla_x \hat{f}(x_t, y_t; z_t), \Delta_t^x \rangle \\ &\quad + \tau_2 \langle (1 + \ell \tau_2 + 2L_\Psi \tau_2) \nabla_y f(x_t, y_t) - 2 \nabla_y f(x^*(y_t, z_t), y_t), \Delta_t^y \rangle, \\ \tilde{D}_{t+1} &\triangleq 2\ell \tau_1^2 \|\Delta_t^x\|^2 + 8\ell \tau_2^2 \|\Delta_t^y\|^2. \end{aligned}$$

Proof. The proof is given in Appendix D. \square

Next, we provide a concentration inequality which will be key to obtain our high-probability bounds.

Theorem 9. Let $\{\mathcal{F}_t\}_{t \in \mathbb{N}}$ be a filtration on $(\Omega, \mathcal{F}, \mathbb{P})$. Let A_t, B_t, C_t, D_t be four stochastic processes adapted to the filtration such that there exist $\sigma_C, \sigma_D > 0$ and $\tau > 0$ such that for all $t \in \mathbb{N}$: (i) $B_t \geq 0$, (ii) $\mathbb{E}[e^{\lambda C_{t+1}} \mid \mathcal{F}_t] \leq e^{\lambda^2 \sigma_C^2 B_t}$ for all $\lambda > 0$, (iii) $\mathbb{E}[e^{\lambda D_{t+1}} \mid \mathcal{F}_t] \leq e^{\lambda \sigma_D^2}$ for all $\lambda \in [0, \frac{1}{\sigma_D^2}]$ and (iv) $\frac{A_{t+1} - A_t}{\tau} \leq -B_t + C_{t+1} + D_{t+1}$. Then, for any $\bar{q} \in (0, 1]$, we have

$$\mathbb{P}\left(\frac{\tau}{2} \sum_{t=0}^{T-1} B_t \leq (A_0 - A_T) + \tau \sigma_D^2 T + 2\tau \max\{2\sigma_C^2, \sigma_D^2\} \log\left(\frac{1}{\bar{q}}\right)\right) \geq 1 - \bar{q}.$$

Proof. The proof is provided in Appendix E. \square

We next present our main result which provides a high-probability bound on the sm-AGDA iterates. The main idea of the proof is to apply Theorem 9 to the processes introduced in Corollary 8.

Theorem 10. In the premise of Corollary 8, sm-AGDA iterates (x_t, y_t) for $\tau_1 = \bar{\tau} \leq \frac{1}{3\ell}$ satisfy

$$\mathbb{P}\left(\frac{1}{T} \sum_{t=0}^{T-1} [\|\nabla_x f(x_t, y_t)\|^2 + \kappa \|\nabla_y f(x_t, y_t)\|^2] \leq \mathcal{Q}_{\bar{q}, T},\right) \geq 1 - \bar{q}, \quad \forall T \in \mathbb{N}, \quad \forall \bar{q} \in (0, 1],$$

for some $\mathcal{Q}_{\bar{q}, T} = \mathcal{O}\left(\frac{\kappa(\Delta_0 + b_0)}{\bar{\tau} T} + \kappa(\delta_x^2 + \delta_y^2)\left(\bar{\tau}\ell + \frac{1}{T} \log\left(\frac{1}{\bar{q}}\right)\right)\right)$ explicitly stated in Appendix F, where $\Delta_0 \triangleq \Phi(z_0) - \Phi^*$, $b_0 \triangleq 2 \sup_{x, y} \{\hat{f}(x_0, y; z_0) - \hat{f}(x, y_0; z_0)\}$.

Proof Sketch. Let A_t, B_t, C_t, D_t stochastic processes and $\tau > 0$ in Theorem 9 be chosen as $A_t = \tilde{A}_t$, $B_t = \tilde{B}_t$, $C_t = \tilde{C}_t$, $D_t = \tilde{D}_t$ and we set $\tau = \tau_1$, where $\tilde{A}_t, \tilde{B}_t, \tilde{C}_t, \tilde{D}_t$ are defined in Corollary 8 and $\tau_1 > 0$ is the primal stepsize in sm-AGDA; thus, according to Corollary 8, we have $\frac{A_{t+1} - A_t}{\tau_1} \leq -B_t + C_{t+1} + D_{t+1}$ for $t \in \mathbb{N}$. Since Δ_t^x and Δ_t^y admit sub-Gaussian tails, it can be shown that the conditions of Theorem 9 are satisfied for some appropriate constants σ_C^2 and σ_D^2 . Therefore, Theorem 9 implies a tail bound on $\sum_{t=0}^{T-1} \tilde{B}_t$. Using the relation between f and \hat{f} , one can also show that $\|\nabla_x f(x_t, y_t)\|^2 + \kappa \|\nabla_y f(x_t, y_t)\|^2 = \mathcal{O}(\tilde{B}_t)$, for all $t \in \mathbb{N}$. This last inequality allows to translate the tail bound for $\sum_{t=0}^{T-1} \tilde{B}_t$ to a tail bound for $\sum_{t=0}^{T-1} \|\nabla_x f(x_t, y_t)\|^2 + \kappa \|\nabla_y f(x_t, y_t)\|^2$. The details of the proof is provided in Appendix F of the Appendix. \square

Remark 11. Suppose sm-AGDA, given in Alg. 1, is run for T iterations, and it outputs a randomly selected iterate (x_U, y_U) , where the random iteration index U is chosen uniformly at random from the set $\{0, 1, \dots, T-1\}$, i.e., $\mathbb{P}(U = t) = 1/T$ for $t = 0, 1, \dots, T-1$. Theorem 10 implies that

$$\mathbb{P}\left(\|\nabla_x f(x_U, y_U)\|^2 + \kappa \|\nabla_y f(x_U, y_U)\|^2 \leq \mathcal{Q}_{\bar{q}, T}\right) \geq 1 - \bar{q}.$$

Furthermore, in comparison with existing complexity bounds in expectation for sm-AGDA [63], our quantile bound requires only an overhead of order $\mathcal{O}(\varepsilon^{-2} \log(1/\bar{q}))$. Unless \bar{q} is very small, this is typically negligible in comparison to the $\mathcal{O}(\varepsilon^{-4})$ already present in rates in expectation.

Corollary 12. Under the premise of Theorem 10, consider running the sm-AGDA method for some fixed number of iterations $T \in \mathbb{N}$ with parameters chosen as $\tau_1 = \bar{\tau}$ and $\tau_2 = \bar{\tau}/48$ for $\bar{\tau} \triangleq \min\left(\frac{1}{3\ell}, \frac{48\sqrt{\Delta_0 + b_0}}{\sqrt{T\ell\delta^2}}\right)$, where $\delta^2 \triangleq \delta_x^2 + \delta_y^2$. Then, for any $\bar{q} \in (0, 1)$, sm-AGDA can compute an $(\varepsilon, \varepsilon/\sqrt{\kappa})$ stationarity point with probability at least $1 - \bar{q}$ when the number of iterations T is fixed to $T_{\varepsilon, \bar{q}} = \mathcal{O}\left(\frac{(\Delta_0 + b_0)\ell\kappa}{\varepsilon^2} + \frac{\delta^2 \log\left(\frac{1}{\bar{q}}\right)\kappa}{\varepsilon^2} + \frac{\delta^2(\Delta_0 + b_0)\ell\kappa^2}{\varepsilon^4}\right)$ which requires $T_{\varepsilon, \bar{q}}$ stochastic gradient calls.

Proof. This is a direct consequence of Theorem 10, a proof is provided in Appendix G. \square

4 Numerical Illustrations

In this section, we illustrate the performance of sm-AGDA. We consider an NCPL problem with synthetic data, as well as a nonconvex DRO problem using real datasets. For synthetic experiments, we used an ASUS Laptop model Q540VJ with 13th Generation Intel Core i9-13900H using 16GB RAM and 1TB SSD hard drive. For the DRO experiments, we used a high-performance computing cluster with automatic GPU selection (NVIDIA RTX 3050, RTX 3090, A100, or Tesla P100) based on GPU availability, ensuring optimal use of computational resources.

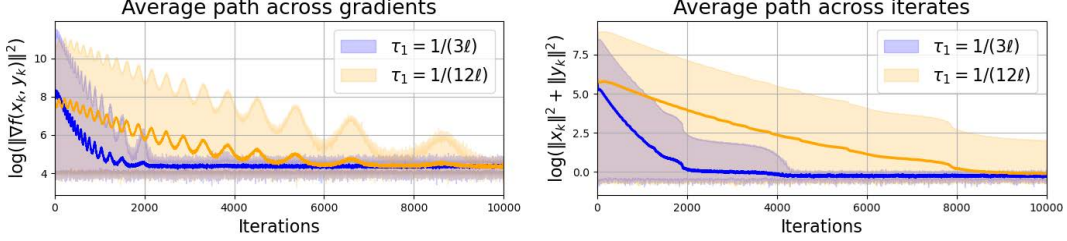


Figure 1: NCPL game with $\tau_1 = \frac{1}{3\ell}$ (long step) and $\tau_1 = \frac{1}{12\ell}$ (short step). (Left) Average of $\mathcal{M}_k(t)$ over 25 sample paths vs. iterations t . (Right) Average of $\mathcal{I}(t)$ over 25 sample paths vs. iterations t . In both plots, shaded regions depict the range statistic over 25 sample paths.

Synthetic experiments on an NCPL game. We consider the following NCPL problem:

$$\max_{x \in \mathbb{R}^{d_1}} \min_{y \in \mathbb{R}^{d_2}} m_1 \left[\|x\|^2 + \sin \left(3\sqrt{\|x\|^2 + 1} \right) \right] + x^\top Ky - m_2 \left[\|y\|^2 + 3\sin^2(\|y\|) \right], \quad (13)$$

which can be interpreted as a game between two players [45, 34] where $m_1, m_2 > 0$ are constants and the symmetric matrix K is set randomly, similar to the standard bilinear game setting considered in [34]. More specifically, we set $K = 10\tilde{K}/\|\tilde{K}\|$, $\tilde{K} = (M + M^\top)/2$ where M is a $d \times d$ matrix with entries being i.i.d centered Gaussian having variance σ^2 . This problem is nonconvex in x (without satisfying the PL condition in x). Though the exact gradient is known, we consider a stochastic gradient oracle, which returns *noisy* gradients similar to the setting of [34, 11, 16, 2], i.e., for each iteration $t \in \{0, \dots, T-1\}$, $G_x(x_t, y_t; \xi_{t+1}^x) = \nabla_x f(x_t, y_t) + \xi_{t+1}^x$ and $G_y(x_{t+1}, y_t, \xi_{t+1}^y) = \nabla_y f(x_{t+1}, y_t) + \xi_{t+1}^y$, with $(\xi_{t+1}^x)_{t \geq 0} \stackrel{iid}{\sim} \mathcal{N}(\mathbf{0}, \delta^2 I_{d_1})$ and $(\xi_{t+1}^y)_{t \geq 0} \stackrel{iid}{\sim} \mathcal{N}(\mathbf{0}, \delta^2 I_{d_2})$ where I_d is the $d \times d$ identity matrix and δ^2 is some constant variance. This setting satisfies all our assumptions, and our high-probability results (Theorem 10 and Coro. 12) are applicable. In this experiment, we fix $d_1 = d_2 = 30$, and $m_1 = m_2 = \delta^2 = \sigma^2 = 1$. The solution to this problem is $(x^*, y^*) = (\mathbf{0}, \mathbf{0})$.

Experimental results. The parameters of the problem are explicitly available as $\mu = 2m_2$, and $\ell = \max\{12m_1, 8m_2, \|K\|\}$. To illustrate Theorem 10, we set $\beta = \frac{\tau_2 \mu}{1600}$, $\tau_2 = \frac{\tau_1}{48}$, $p = 2\ell$ and we considered two cases: $\tau_1 = \frac{1}{3\ell}$ (long step) and $\tau_1 = \frac{1}{12\ell}$ (short step) to explore the behavior of sm-AGDA for different stepsizes. We generated $N = 25$ sample paths for $T = 10,000$ iterations, and on the left panel of Fig. 1, for each iteration t , we report the average of $\mathcal{M}_k(t) \triangleq \|\nabla_x f(x_t, y_t)\|^2 + \kappa \|\nabla_y f(x_t, y_t)\|^2$ over $N = 25$ realizations corresponding to different sample paths, and the shaded region depicts the range statistic, i.e., for every fixed iteration t , we shade the vertical line between the maximum and minimum values of $\mathcal{M}_k(t)$ for the 25 paths. On the right panel of Fig. 1, we also report the squared distance, $\mathcal{I}(t) \triangleq \|x_t - x^*\|^2 + \|y_t - y^*\|^2$, in a similar manner. We observe that the range statistic for $\mathcal{M}_k(t)$ diminishes to a value inversely proportional to T as $t \rightarrow T$; this is inline with our theoretical results in Theorem 10. The existence of sinusoidal terms in the minimax objective is a source for oscillatory behavior in these figures. As $t \rightarrow T$, both $\mathcal{M}_k(t)$ and $\mathcal{I}(t)$ exhibit oscillations, of which amplitude are smaller for the small step size compared to the large step-size –at the expense of a slower convergence; the iterate paths are not as oscillatory.

For $T = 10,000$ and $\tau_1 = \frac{1}{3\ell}$ fixed, we next consider the path averages $X_T \triangleq \frac{1}{T} \sum_{t=0}^{T-1} \mathcal{M}_k(t)$. Indeed, based on 1000 sample paths, each for $T = 10,000$ iterations, we compare the empirical quantiles of X_T with the theoretical upper bound $\mathcal{Q}_{q,T}$ on its quantiles (implied by Theorem 10). Figure 2 shows the cumulative distribution function (CDF) of the empirical distribution alongside the theoretical explicit upper bound $\mathcal{Q}_{q,T}$ for the stationarity measure $\|\nabla_x f(x_U, y_U) + \kappa \nabla_y f(x_U, y_U)\|$ with U uniform over $\{1, \dots, T\}$. The details of the empirical quantile estimation are provided Appendix I due to space considerations. We observe that the empirical CDF has a sigmoid-like shape, while the theoretical quantiles that lie above display a concave form. This difference may arise because

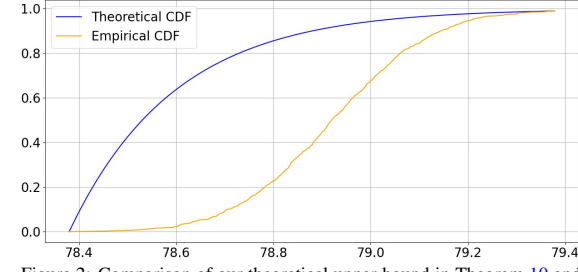


Figure 2: Comparison of our theoretical upper bound in Theorem 10 and the empirical stationarity measure of sm-AGDA for Problem (13). Results are reported as cumulative distribution functions.

the theoretical quantile bounds $\mathcal{Q}_{q,T}$ are designed to capture the worst-case behavior across the class of NCPL problems, whereas this specific NCPL example may not represent the worst-case scenario.

Distributionally Robust nonconvex Logistic Regression. We consider the DRO problem

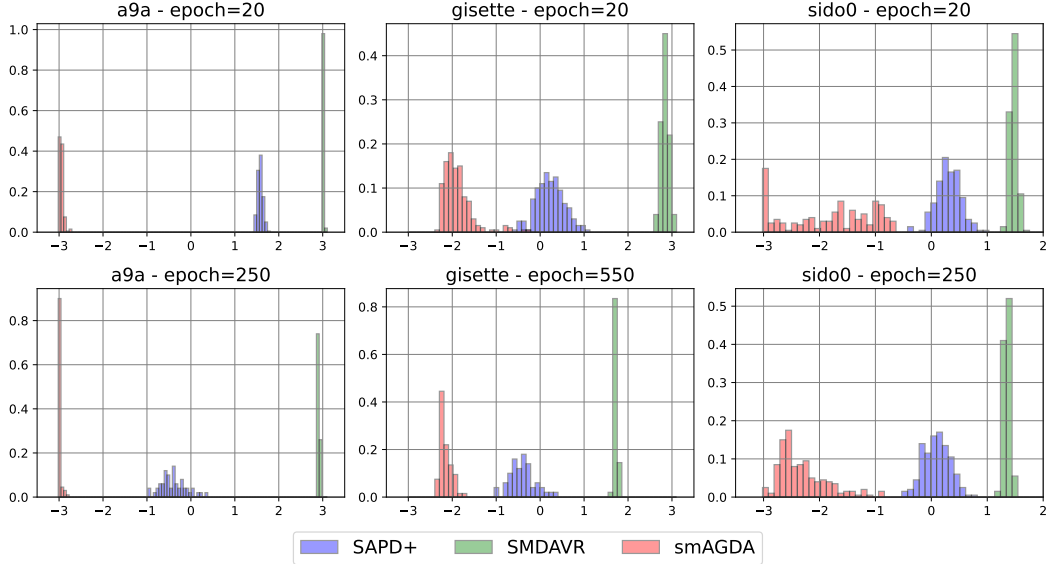


Figure 3: Histograms for the stationarity measure $\log_{10} \|\nabla f(x_t, y_t)\|^2$ for sm-AGDA and baseline algorithms (SAPD+, SMDA, and SMDAVR) on a9a, gisette, and sido0 datasets. Each algorithm is run 200 times. First row reports histograms after 20 epochs, and second row reports histograms at the end of training.

$$\min_{x \in \mathbb{R}^{d_1}} \max_{y \in Y} \left(\frac{1}{d_2} \sum_{j=1}^{d_2} y_j \ell_j(x; a_j, b_j) + r(x) - g(y) \right), \quad (14)$$

where $\ell_j(x; a_j, b_j) = \log(1 + \exp(-b_j \mathbf{a}_j^\top \mathbf{x}))$ denotes the logistic loss tied to an input-output pair $(a_j, b_j) \in \mathbb{R}^{d_1} \times \{-1, 1\}$, and $r(x) = \lambda_1 \sum_{i=1}^{d_1} \frac{\omega_i}{1 + \omega_i x_i^2}$ a primal regularization for the learning model $x \in \mathbb{R}^{d_1}$. We allow the distribution $y \in Y \triangleq \{y \in \mathbb{R}^{d_2} : y \geq 0, \mathbf{1}^\top y = 1\}$ to deviate from the uniform distribution $u \triangleq \frac{1}{d_2} \mathbf{1}$ where $\mathbf{1}$ denotes the vector of ones, and we penalize the distance between y and u through the regularization map $g : y \mapsto \frac{\lambda_2 d_2}{2} \|y - u\|^2$. We set the regularization parameters as $\omega = 10$, $\lambda_1 = 10e^{-4}$, and $\lambda_2 = 1$. Since r is nonconvex with a Lipschitz gradient and g is strongly convex, this is an NCSC problem.

Datasets, Algorithms and Hyperparameters. We consider three standard datasets for this problem, which are summarized as follows: The sido0 dataset [47] has $d_1 = 4932$ and $d_2 = 12678$. The gisette dataset [26] has $d_1 = 5000$ and $d_2 = 6000$. Finally, the a9a dataset [13] has $d_1 = 123$ and $d_2 = 32561$. We compare the performances of sm-AGDA against two other baselines that achieve state-of-the-art performance in expectation for these datasets [69]. Specifically, we evaluate SAPD+, which is a two-loop method where the subproblems are solved by the SAPD algorithm [70], and SMDAVR, a variance reduced extension of SMDA algorithm [30]. Since (14) is constrained, we augment sm-AGDA with a projection step in the update of the y variable onto the d_2 -dimensional simplex and adopt the analogous stationarity metric $\|\nabla_x f(x_t, y_t)\|^2 + \|P_Y \nabla_y f(x_t, y_t)\|^2$ for constrained problems where P_Y is a projection to the dual domain Y . For all datasets, the primal stepsize τ_1 of sm-AGDA is tuned via a grid-search over $\{10^{-k}, 1 \leq k \leq 4\}$. The dual stepsize τ_2 is set as $\tau_2 = \frac{\tau_1}{48}$. Similarly, β is estimated through a grid-search over $\{10^{-k}, 3 \leq k \leq 5\}$. The parameter p is also tuned similarly on a grid. For other methods, our hyperparameters are tuned in accordance with [69].

Experimental results. In Figure 2, we plot histograms of our stationarity metric, across 200 runs in a logarithmic scale. We report the stationarity measure both in early phase of the training (i.e. $t = 20$ epochs), and in later phases (i.e. $t = 550$ epochs for gisette and $t = 250$ epochs for a9a and sido0). Our theoretical results are presented for unconstrained problems in the dual, therefore they are not directly applicable to the DRO problem where the dual domain is constrained. That being said, we observe that they are still predictive of performance in the DRO setting. More specifically, Figure 2 is supportive of our high-probability complexity bounds for sm-AGDA, in the sense that the distribution of the stationarity metric for sm-AGDA tends to concentrate. Notably, it outperforms the concentration behaviour of the other baselines. Furthermore, we observe that histograms for all baselines hardly evolve after 20 epochs. This is consistent with previous experiments carried on these datasets [69] where performance was measured in terms of the decay of the average loss and its standard deviation. As such, we conclude that sm-AGDA performs better both in the early phase and the later stage. In our experience, we observed sm-AGDA could accommodate larger stepsizes compared to the other algorithms, which may have contributed to its good performance.

5 Conclusion

Existing high-probability bounds only apply to convex/concave minimax problems or non-monotone variational inequality problems under restrictive assumptions to our knowledge. We close this gap by providing the first high-probability complexity guarantees for nonconvex/PL minimax problems satisfying the PL-condition in the dual variable for the sm-AGDA method. We also provide numerical results for an NCPL example and for nonconvex distributionally robust logistic regression.

Acknowledgements

Yassine Laguel, Yasa Syed and Mert Gürbüzbalaban's research are supported in part by the grants Office of Naval Research Award Number N00014-21-1-2244, National Science Foundation (NSF) CCF-1814888 and NSF DMS-2053485. Necdet Serhat Aybat's work was supported in part by the grant Office of Naval Research Award N00014-21-1-2271.

References

- [1] Jason Altschuler and Kunal Talwar. Privacy of noisy stochastic gradient descent: More iterations without more privacy loss. *Advances in Neural Information Processing Systems*, 35:3788–3800, 2022.
- [2] Necdet Serhat Aybat, Alireza Fallah, Mert Gurbuzbalaban, and Asuman Ozdaglar. Robust accelerated gradient methods for smooth strongly convex functions. *SIAM Journal on Optimization*, 30(1):717–751, 2020.
- [3] Amir Beck and Aharon Ben-Tal. Duality in robust optimization: primal worst equals dual best. *Operations Research Letters*, 37(1):1–6, 2009.
- [4] Aharon Ben-Tal, Laurent El Ghaoui, and Arkadi Nemirovski. *Robust Optimization*, volume 28. Princeton University Press, 2009.
- [5] Aleksandr Beznosikov, Boris Polyak, Eduard Gorbunov, Dmitry Kovalev, and Alexander Gasnikov. Smooth monotone stochastic variational inequalities and saddle point problems: A survey. *European Mathematical Society Magazine*, (127):15–28, 2023.
- [6] Radu Ioan Boț and Axel Böhm. Alternating proximal-gradient steps for (stochastic) nonconvex-concave minimax problems. *arXiv preprint arXiv:2007.13605*, 2020.
- [7] Radu Ioan Boț, Panayotis Mertikopoulos, Mathias Staudigl, and Phan Tu Vuong. Minibatch forward-backward-forward methods for solving stochastic variational inequalities. *Stochastic Systems*, 11(2):112–139, 2021.
- [8] Léon Bottou. Large-scale machine learning with stochastic gradient descent. In *Proceedings of COMPSTAT'2010*, pages 177–186. Springer, 2010.
- [9] Léon Bottou, Frank E Curtis, and Jorge Nocedal. Optimization methods for large-scale machine learning. *SIAM Review*, 60(2):223–311, 2018.
- [10] Nicolas Boumal and Pierre-antoine Absil. Rtrmc: A Riemannian trust-region method for low-rank matrix completion. *Advances in Neural Information Processing Systems*, 24, 2011.
- [11] Bugra Can, Mert Gurbuzbalaban, and Lingjiong Zhu. Accelerated linear convergence of stochastic momentum methods in Wasserstein distances. In *International Conference on Machine Learning*, pages 891–901. PMLR, 2019.
- [12] Antonin Chambolle and Thomas Pock. A first-order primal-dual algorithm for convex problems with applications to imaging. *Journal of mathematical imaging and vision*, 40:120–145, 2011.
- [13] Chih-Chung Chang and Chih-Jen Lin. LIBSVM: a library for support vector machines. *ACM Transactions on Intelligent Systems and Technology (TIST)*, 2(3):1–27, 2011.
- [14] Rishav Chourasia, Jiayuan Ye, and Reza Shokri. Differential privacy dynamics of Langevin diffusion and noisy gradient descent. *Advances in Neural Information Processing Systems*, 34:14771–14781, 2021.
- [15] Constantinos Daskalakis, Dylan J Foster, and Noah Golowich. Independent policy gradient methods for competitive reinforcement learning. *Advances in Neural Information Processing Systems*, 33:5527–5540, 2020.
- [16] Alireza Fallah, Asuman Ozdaglar, and Sarath Pattathil. An optimal multistage stochastic gradient method for minimax problems. In *2020 59th IEEE Conference on Decision and Control (CDC)*, pages 3573–3579. IEEE, 2020.
- [17] Maryam Fazel, Rong Ge, Sham Kakade, and Mehran Mesbahi. Global convergence of policy gradient methods for the linear quadratic regulator. In *International Conference on Machine Learning*, pages 1467–1476. PMLR, 2018.

[18] Saeed Ghadimi and Guanghui Lan. Optimal stochastic approximation algorithms for strongly convex stochastic composite optimization I: A generic algorithmic framework. *SIAM Journal on Optimization*, 22(4):1469–1492, 2012.

[19] Saeed Ghadimi and Guanghui Lan. Stochastic first-and zeroth-order methods for nonconvex stochastic programming. *SIAM Journal on Optimization*, 23(4):2341–2368, 2013.

[20] Eduard Gorbunov, Marina Danilova, David Dobre, Pavel Dvurechenskii, Alexander Gasnikov, and Gauthier Gidel. Clipped stochastic methods for variational inequalities with heavy-tailed noise. In S. Koyejo, S. Mohamed, A. Agarwal, D. Belgrave, K. Cho, and A. Oh, editors, *Advances in Neural Information Processing Systems*, volume 35, pages 31319–31332, 2022.

[21] Eduard Gorbunov, Nicolas Loizou, and Gauthier Gidel. Extragradient method: $\mathcal{O}(1/k)$ last-iterate convergence for monotone variational inequalities and connections with cocoercivity. In *International Conference on Artificial Intelligence and Statistics*, pages 366–402, 2022.

[22] Eduard Gorbunov, Abdurakhmon Sadiev, Marina Danilova, Samuel Horváth, Gauthier Gidel, Pavel Dvurechensky, Alexander Gasnikov, and Peter Richtárik. High-probability convergence for composite and distributed stochastic minimization and variational inequalities with heavy-tailed noise. *arXiv preprint arXiv:2310.01860*, 2023.

[23] Mert Gürbüzbalaban, Yuanhan Hu, Umut Simsekli, and Lingjiong Zhu. Cyclic and randomized stepsizes invoke heavier tails in SGD than constant stepsize. *Transactions on Machine Learning Research*, August 2023.

[24] Mert Gürbüzbalaban, Andrzej Ruszczyński, and Landi Zhu. A stochastic subgradient method for distributionally robust non-convex and non-smooth learning. *Journal of Optimization Theory and Applications*, 194(3):1014–1041, 2022.

[25] Mert Gürbüzbalaban, Umut Simsekli, and Lingjiong Zhu. The heavy-tail phenomenon in SGD. In *International Conference on Machine Learning*, pages 3964–3975. PMLR, 2021.

[26] Isabelle Guyon, Steve Gunn, Asa Ben-Hur, and Gideon Dror. Result analysis of the NIPS2003 feature selection challenge. *Advances in Neural Information Processing Systems*, 17, 2004.

[27] Mark Herbster, Stephen Pasteris, and Lisa Tse. Online matrix completion with side information. *Advances in Neural Information Processing Systems*, 33:20402–20414, 2020.

[28] Yu-Guan Hsieh, Franck Iutzeler, Jérôme Malick, and Panayotis Mertikopoulos. On the convergence of single-call stochastic extra-gradient methods. *Advances in Neural Information Processing Systems*, 32, 2019.

[29] Feihu Huang, Shangqian Gao, Jian Pei, and Heng Huang. Accelerated zeroth-order and first-order momentum methods from mini to minimax optimization. *Journal of Machine Learning Research*, 23(36):1–70, 2022.

[30] Feihu Huang, Xidong Wu, and Heng Huang. Efficient mirror descent ascent methods for nonsmooth minimax problems. *Advances in Neural Information Processing Systems*, 34, 2021.

[31] Anatoli Juditsky, Arkadi Nemirovski, and Claire Tauvel. Solving variational inequalities with stochastic mirror-prox algorithm. *Stochastic Systems*, 1(1):17–58, 2011.

[32] Yang Junchi, Xiang Li, and Niao He. Nest your adaptive algorithm for parameter-agnostic nonconvex minimax optimization. In *Advances in Neural Information Processing Systems*, 2022.

[33] Nurdan Kuru, Ş. İlker Birbil, Mert Gürbüzbalaban, and Sinan Yıldırım. Differentially private accelerated optimization algorithms. *SIAM Journal on Optimization*, 32(2):795–821, 2022.

[34] Yassine Laguel, Necdet Serhat Aybat, and Mert Gürbüzbalaban. High probability and risk-averse guarantees for stochastic saddle point problems. *arXiv preprint arXiv:2304.00444*, 2023.

[35] Guanghui Lan. *First-order and stochastic optimization methods for machine learning*, volume 1. Springer, 2020.

[36] Dongyang Li, Haobin Li, and Junyu Zhang. General procedure to provide high-probability guarantees for stochastic saddle point problems. *arXiv preprint arXiv:2405.03219*, 2024.

[37] Haochuan Li, Yi Tian, Jingzhao Zhang, and Ali Jadbabaie. Complexity lower bounds for nonconvex-strongly-concave min-max optimization. *Advances in Neural Information Processing Systems*, 34:1792–1804, 2021.

[38] Tianyi Lin, Chi Jin, and Michael Jordan. On gradient descent ascent for nonconvex-concave minimax problems. In *International Conference on Machine Learning*, pages 6083–6093. PMLR, 2020.

[39] Tianyi Lin, Chi Jin, and Michael I Jordan. Near-optimal algorithms for minimax optimization. In *Conference on Learning Theory*, pages 2738–2779. PMLR, 2020.

[40] Chaoyue Liu, Libin Zhu, and Mikhail Belkin. Loss landscapes and optimization in over-parameterized non-linear systems and neural networks. *Applied and Computational Harmonic Analysis*, 59:85–116, 2022. Special Issue on Harmonic Analysis and Machine Learning.

[41] Aleksander Madry, Aleksandar Makelov, Ludwig Schmidt, Dimitris Tsipras, and Adrian Vladu. Towards deep learning models resistant to adversarial attacks. *arXiv preprint arXiv:1706.06083*, 2017.

[42] Gabriel Mancino-Ball and Yangyang Xu. Variance-reduced accelerated methods for decentralized stochastic double-regularized nonconvex strongly-concave minimax problems. *arXiv preprint arXiv:2307.07113*, 2023.

[43] Hongseok Namkoong and John C Duchi. Stochastic gradient methods for distributionally robust optimization with f-divergences. In *Advances in Neural Information Processing Systems*, pages 2208–2216, 2016.

[44] Angelia Nedić and Tatiana Tütüncü. Huber loss-based penalty approach to problems with linear constraints. *arXiv preprint arXiv:2311.00874*, 2023.

[45] Maher Nouiehed, Maziar Sanjabi, Tianjian Huang, Jason D Lee, and Meisam Razaviyayn. Solving a class of non-convex min–max games using iterative first order methods. *Advances in Neural Information Processing Systems*, 32, 2019.

[46] Balamurugan Palaniappan and Francis Bach. Stochastic variance reduction methods for saddle-point problems. In *Advances in Neural Information Processing Systems*, pages 1416–1424, 2016.

[47] DTP AIDS Antiviral Screen program. Sido0: a pharmacology dataset. <https://www.causality.inf.ethz.ch/data/SIDO.html>, 2008.

[48] H Rafique, M Liu, Q Lin, and T Yang. Non-convex min–max optimization: provable algorithms and applications in machine learning (2018). *arXiv preprint arXiv:1810.02060*, 1810.

[49] Harish Rajagopal. Multistage step size scheduling for minimax problems. Master’s thesis, ETH Zurich. URL: <https://www.research-collection.ethz.ch/handle/20.500.11850/572991>, 2022.

[50] Meisam Razaviyayn, Tianjian Huang, Songtao Lu, Maher Nouiehed, Maziar Sanjabi, and Mingyi Hong. Nonconvex min–max optimization: Applications, challenges, and recent theoretical advances. *IEEE Signal Processing Magazine*, 37(5):55–66, 2020.

[51] Abdurakhmon Sadiev, Marina Danilova, Eduard Gorbunov, Samuel Horváth, Gauthier Gidel, Pavel Dvurechensky, Alexander Gasnikov, and Peter Richtárik. High-probability bounds for stochastic optimization and variational inequalities: the case of unbounded variance. In *International Conference on Machine Learning*, pages 29563–29648. PMLR, 2023.

[52] Umut Simsekli, Levent Sagun, and Mert Gürbüzbalaban. A tail-index analysis of stochastic gradient noise in deep neural networks. In *International Conference on Machine Learning*, pages 5827–5837. PMLR, 2019.

[53] Ju Sun, Qing Qu, and John Wright. Complete dictionary recovery over the sphere ii: Recovery by riemannian trust-region method. *IEEE Transactions on Information Theory*, 63(2):885–914, 2017.

[54] J v. Neumann. Zur theorie der gesellschaftsspiele. *Mathematische Annalen*, 100(1):295–320, 1928.

[55] Emmanouil-Vasileios Vlatakis-Gkaragkounis, Lampros Flokas, and Georgios Piliouras. Solving min–max optimization with hidden structure via gradient descent ascent. *Advances in Neural Information Processing Systems*, 34:2373–2386, 2021.

[56] Yuanhao Wang and Jian Li. Improved algorithms for convex-concave minimax optimization. *Advances in Neural Information Processing Systems*, 33:4800–4810, 2020.

[57] Linli Xu, James Neufeld, Bryce Larson, and Dale Schuurmans. Maximum margin clustering. In *Advances in Neural Information Processing systems*, pages 1537–1544, 2005.

[58] Qiushui Xu, Xuan Zhang, Necdet Serhat Aybat, and Mert Gürbüzbalaban. A stochastic gda method with backtracking for solving nonconvex (strongly) concave minimax problems. *arXiv preprint arXiv:2403.07806*, 2024.

[59] Qiushui Xu, Xuan Zhang, Necdet Serhat Aybat, and Mert Gürbüzbalaban. A Stochastic GDA Method With Backtracking For Solving Nonconvex (Strongly) Concave Minimax Problems. *arXiv e-prints*, page arXiv:2403.07806, March 2024.

[60] Yan Yan, Yi Xu, Qihang Lin, Wei Liu, and Tianbao Yang. Optimal epoch stochastic gradient descent ascent methods for min–max optimization. In H. Larochelle, M. Ranzato, R. Hadsell, M.F. Balcan, and H. Lin, editors, *Advances in Neural Information Processing Systems*, volume 33, pages 5789–5800, 2020.

[61] Junchi Yang, Negar Kiyavash, and Niao He. Global convergence and variance reduction for a class of nonconvex-nonconcave minimax problems. *Advances in Neural Information Processing Systems*, 33:1153–1165, 2020.

- [62] Junchi Yang, Antonio Orvieto, Aurelien Lucchi, and Niao He. Faster single-loop algorithms for minimax optimization without strong concavity. In *International Conference on Artificial Intelligence and Statistics*, pages 5485–5517. PMLR, 2022.
- [63] Junchi Yang, Antonio Orvieto, Aurelien Lucchi, and Niao He. Faster single-loop algorithms for minimax optimization without strong concavity. In *International Conference on Artificial Intelligence and Statistics*, pages 5485–5517. PMLR, 2022.
- [64] TaeHo Yoon and Ernest K Ryu. Accelerated minimax algorithms flock together. *arXiv preprint arXiv:2205.11093*, 2022.
- [65] Zhuoning Yuan, Yan Yan, Milan Sonka, and Tianbao Yang. Large-scale robust deep auc maximization: A new surrogate loss and empirical studies on medical image classification. In *Proceedings of the IEEE/CVF International Conference on Computer Vision*, pages 3040–3049, 2021.
- [66] Yuxuan Zeng, Zhiguo Wang, Jianchao Bai, and Xiaojing Shen. An accelerated stochastic ADMM for nonconvex and nonsmooth finite-sum optimization. *arXiv preprint arXiv:2306.05899*, 2023.
- [67] Jiawei Zhang, Peijun Xiao, Ruoyu Sun, and Zhiqian Luo. A single-loop smoothed gradient descent-ascent algorithm for nonconvex-concave min-max problems. *Advances in Neural Information Processing Systems*, 33:7377–7389, 2020.
- [68] Siqi Zhang, Junchi Yang, Cristóbal Guzmán, Negar Kiyavash, and Niao He. The complexity of nonconvex-strongly-concave minimax optimization. In *Uncertainty in Artificial Intelligence*, pages 482–492. PMLR, 2021.
- [69] Xuan Zhang, Necdet Serhat Aybat, and Mert Gürbüzbalaban. SAPD+: An accelerated stochastic method for nonconvex-concave minimax problems. *Advances in Neural Information Processing Systems*, 35:21668–21681, 2022.
- [70] Xuan Zhang, Necdet Serhat Aybat, and Mert Gürbüzbalaban. Robust accelerated primal-dual methods for computing saddle points. *SIAM Journal on Optimization*, 34(1):1097–1130, 2024.
- [71] Yuchen Zhang and Lin Xiao. Stochastic primal-dual coordinate method for regularized empirical risk minimization. *The Journal of Machine Learning Research*, 18(1):2939–2980, 2017.
- [72] Landi Zhu, Mert Gürbüzbalaban, and Andrzej Ruszczyński. Distributionally robust learning with weakly convex losses: Convergence rates and finite-sample guarantees. *arXiv preprint arXiv:2301.06619*, 2023.

High-probability complexity guarantees for nonconvex minimax problems

APPENDIX

The organization of the Appendix is as follows:

- In Section A, we summarize the key notations that are used throughout the main paper and the Appendix.
- In Section B, we provide the proofs of Lemmas from Section 3 that were used for deriving the approximate Lyapunov descent property.
- In Section C, we present the proof of Theorem 7 which provides an approximate descent property in terms of the Lyapunov function for the sm-AGDA iterates.
- In Section D, we provide the proof of Corollary 8, which studies particular choice of parameters within Theorem 7.
- In Section E we present a proof of Theorem 9 which provides a concentration inequality.
- In Section F, we provide the proof of Theorem 10 which yields high-probability results for the sm-AGDA algorithm.
- In Section G, we provide a proof of Corollary 12 that provides a high-probability (iteration) complexity bound for the sm-AGDA iterates.
- In Section H, we present supplementary lemmas that were used to derive the results.
- In Section I, we provide further details about numerical experiments.

A Notation

The key notations that will be used throughout the Appendix is as follows:

- $\hat{f}(x, y; z) = f(x, y) + \frac{p}{2} \|x - z\|^2$ denotes the auxiliary problem.
- $\Psi(y; z) = \min_x \hat{f}(x, y; z)$ is the dual function of the auxiliary problem.
- $\Phi(x; z) = \max_y \hat{f}(x, y; z)$ is the primal function of the auxiliary problem.
- $P(z) = \min_x \max_y \hat{f}(x, y; z)$ is the optimal value of the primal problem $\min_x \Phi(x; z)$
- $x^*(y, z) = \operatorname{argmin}_x \hat{f}(x, y; z)$ for given y, z in the auxiliary function.
- $x^*(z) = \operatorname{argmin}_x \Phi(x; z)$ is the unique optimal solution to the auxiliary primal problem.
- $Y^*(z) = \operatorname{argmax}_y \Psi(y; z)$ is the set of optimal solutions to the auxiliary dual problem.
- $y^+(z) = y + \tau_2 \nabla_y f(x^*(y, z), y)$ denotes an update in y in the direction of the gradient of the dual function, i.e., along the direction $\nabla \Psi(y; z) = \nabla_y f(x^*(y, z), y)$.
- $\hat{G}_x(x, y, \xi; z) \triangleq G_x(x, y, \xi) + p(x - z)$
- $\Delta_t^x = G_x(x_t, y_t, \xi_{t+1}^x) - \nabla_x f(x_t, y_t)$ and $\Delta_t^y = G_y(x_{t+1}, y_t, \xi_{t+1}^y) - \nabla_y f(x_{t+1}, y_t)$ denote the gradient error, i.e., the difference between the stochastic estimates of the partial gradients and the exact partial gradients.

B Proofs of Lemmas from Section 3

B.1 Proof of Lemma 5

Lemma 5. *Suppose Assumptions 1, 2 and 3 hold. Consider sm-AGDA , stated in Algorithm 1, with $\tau_1 \in (0, \frac{1}{p+\ell}]$ and $\beta \in (0, 1]$. For any $t \in \mathbb{N}$, we have:*

$$\begin{aligned}
& \hat{f}(x_{t+1}, y_{t+1}; z_{t+1}) - \hat{f}(x_t, y_t; z_t) \\
& \leq -\frac{\tau_1}{2} \|\nabla_x \hat{f}(x_t, y_t; z_t)\|^2 + \tau_2 \left(1 + \frac{\ell}{2} \tau_2\right) \|\nabla_y f(x_{t+1}, y_t)\|^2 - \frac{p}{2\beta} \|z_t - z_{t+1}\|^2 \\
& \quad + \tau_1((p + \ell)\tau_1 - 1) \langle \Delta_t^x, \nabla_x \hat{f}(x_t, y_t; z_t) \rangle + \tau_2(1 + \ell\tau_2) \langle \Delta_t^y, \nabla_y f(x_{t+1}, y_t) \rangle \\
& \quad + \frac{p + \ell}{2} \tau_1^2 \|\Delta_t^x\|^2 + \frac{\ell\tau_2^2}{2} \|\Delta_t^y\|^2.
\end{aligned}$$

Proof. Since, $\hat{f}(\cdot, y; z)$ is $(p + \ell)$ -smooth, we have

$$\begin{aligned}
& \hat{f}(x_{t+1}, y_t; z_t) - \hat{f}(x_t, y_t; z_t) \\
& \leq \langle x_{t+1} - x_t, \nabla_x \hat{f}(x_t, y_t; z_t) \rangle + \frac{p + \ell}{2} \|x_{t+1} - x_t\|^2 \\
& = -\tau_1 \langle \hat{G}_x(x_t, y_t; z_t), \nabla_x \hat{f}(x_t, y_t; z_t) \rangle + \frac{p + \ell}{2} \tau_1^2 \|\hat{G}_x(x_t, y_t; z_t)\|^2 \\
& = \left(\frac{p + \ell}{2} \tau_1^2 - \tau_1 \right) \|\nabla_x \hat{f}(x_t, y_t; z_t)\|^2 - (\tau_1 + (p + \ell) \tau_1^2) \langle \Delta_t^x, \nabla_x \hat{f}(x_t, y_t; z_t) \rangle \\
& \quad + \frac{p + \ell}{2} \|\Delta_t^x\|^2,
\end{aligned}$$

where last equality follows from $\hat{G}_x(x_t, y_t; z_t) = \nabla_x \hat{f}(x_t, y_t; z_t) + \Delta_t^x$. Hence, for $\tau_1 \leq \frac{1}{p + \ell}$, we have

$$\begin{aligned}
& \hat{f}(x_{t+1}, y_t; z_t) - \hat{f}(x_t, y_t; z_t) \\
& \leq -\frac{\tau_1}{2} \|\nabla_x \hat{f}(x_t, y_t; z_t)\|^2 + \tau_1((p + \ell) \tau_1 - 1) \langle \Delta_t^x, \nabla_x \hat{f}(x_t, y_t; z_t) \rangle + \frac{p + \ell}{2} \tau_1^2 \|\Delta_t^x\|^2. \tag{15}
\end{aligned}$$

Similarly, we observe that for all, $\nabla_y \hat{f}(x, y; z) = \nabla_y f(x, y)$, for all x, y, z , which together with the smoothness of $f(x, \cdot)$ implies

$$\begin{aligned}
& \hat{f}(x_{t+1}, y_{t+1}; z_t) - \hat{f}(x_{t+1}, y_t; z_t) \\
& \leq \langle \nabla_y \hat{f}(x_{t+1}, y_t; z_t), y_{t+1} - y_t \rangle + \frac{\ell}{2} \|y_{t+1} - y_t\|^2 \\
& = \tau_2 \langle \nabla_y f(x_{t+1}, y_t), G_y(x_{t+1}, y_t, \xi_{t+1}^y) \rangle + \frac{\ell}{2} \tau_2^2 \|G_y(x_{t+1}, y_t, \xi_{t+1}^y)\|^2 \\
& = \tau_2 \left(1 + \frac{\ell}{2} \tau_2 \right) \|\nabla_y f(x_{t+1}, y_t)\|^2 + \tau_2(1 + \ell \tau_2) \langle \nabla_y f(x_{t+1}, y_t), \Delta_t^y \rangle + \frac{\ell \tau_2^2}{2} \|\Delta_t^y\|^2,
\end{aligned} \tag{16}$$

where we used again the identity $G_y(x_{t+1}, y_t, \xi_{t+1}^y) = \nabla_y \hat{f}(x_{t+1}, y_t; z_t) + \Delta_t^y$.

Finally, we observe from the **sm-AGDA** update rule $z_{t+1} - z_t = \beta(x_{t+1} - z_t)$ that $\frac{1}{\beta}(z_{t+1} - z_t) = x_{t+1} - z_t$ and $(1 - \beta)(x_{t+1} - z_t) = (x_{t+1} - z_t) - (z_{t+1} - z_t) = x_{t+1} - z_{t+1}$. This gives

$$\begin{aligned}
& \hat{f}(x_{t+1}, y_{t+1}; z_{t+1}) - \hat{f}(x_{t+1}, y_{t+1}; z_t) = \frac{p}{2} [\|x_{t+1} - z_{t+1}\|^2 - \|x_{t+1} - z_t\|^2] \\
& = \frac{p}{2} \left[\|(1 - \beta)(x_{t+1} - z_t)\|^2 - \frac{1}{\beta^2} \|z_{t+1} - z_t\|^2 \right] \\
& = \frac{p}{2} \left[\frac{(1 - \beta)^2}{\beta^2} \|z_{t+1} - z_t\|^2 - \frac{1}{\beta^2} \|z_{t+1} - z_t\|^2 \right] \\
& \leq \frac{-p}{2\beta} \|z_t - z_{t+1}\|^2,
\end{aligned} \tag{17}$$

where we used $0 < \beta \leq 1$. Therefore, summing up (15), (16), (17) yields the claim. \square

B.2 Proof of Lemma 6

Lemma 6. Suppose Assumptions 1, 2 and 3 hold, and $p \geq \ell$. Then, for any $t \in \mathbb{N}$,

$$\begin{aligned}
\Psi(y_{t+1}; z_{t+1}) - \Psi(y_t; z_t) & \geq \tau_2 \langle \nabla_y f(x^*(y_t, z_t), y_t), \nabla_y f(x_{t+1}, y_t) \rangle + \tau_2 \langle \nabla_y f(x^*(y_t, z_t), y_t), \Delta_t^y \rangle \\
& \quad - \frac{L_\Psi}{2} \tau_2^2 (\|\nabla_y f(x_{t+1}, y_t)\|^2 + 2 \langle \nabla_y f(x_{t+1}, y_t), \Delta_t^y \rangle + \|\Delta_t^y\|^2) \\
& \quad + \frac{p}{2} \langle z_{t+1} - z_t, z_{t+1} + z_t - 2x^*(y_{t+1}, z_{t+1}) \rangle,
\end{aligned}$$

where $L_\Psi \triangleq \ell \left(1 + \frac{p + \ell}{p - \ell} \right)$ and the map $x^*(\cdot, \cdot)$ is defined in (11).

Proof. By Lemma 17, Ψ is L_Ψ -smooth in y for any given $z \in \mathbb{R}^{d_1}$. Then, using $\nabla_y \Psi(y_t; z_t) = \nabla_y f(x^*(y_t, z_t), y_t)$, we obtain

$$\begin{aligned}
\Psi(y_{t+1}, z_t) - \Psi(y_t, z_t) & \geq \langle \nabla_y f(x^*(y_t, z_t), y_t; z_t), y_{t+1} - y_t \rangle - \frac{L_\Psi}{2} \|y_{t+1} - y_t\|^2 \\
& \geq \tau_2 \langle \nabla_y f(x^*(y_t, z_t), y_t), \nabla_y f(x_{t+1}, y_t) \rangle + \tau_2 \langle \nabla_y f(x^*(y_t, z_t), y_t), \Delta_t^y \rangle \tag{18} \\
& \quad - \frac{L_\Psi}{2} \tau_2^2 (\|\nabla_y f(x_{t+1}, y_t)\|^2 + 2 \langle \nabla_y f(x_{t+1}, y_t), \Delta_t^y \rangle + \|\Delta_t^y\|^2).
\end{aligned}$$

Furthermore, by definition of Ψ , we also have

$$\begin{aligned}
\Psi(y_{t+1}; z_{t+1}) - \Psi(y_t; z_t) &= \hat{f}(x^*(y_{t+1}, z_{t+1}), y_{t+1}; z_{t+1}) - \hat{f}(x^*(y_t, z_t), y_t; z_t) \\
&\geq \hat{f}(x^*(y_{t+1}, z_{t+1}), y_{t+1}; z_{t+1}) - \hat{f}(x^*(y_t, z_t), y_t; z_t) \\
&= \frac{p}{2} [\|z_{t+1} - x^*(y_{t+1}, z_{t+1})\|^2 - \|z_t - x^*(y_t, z_t)\|^2] \\
&= \frac{p}{2} (z_{t+1} - z_t)^\top [z_{t+1} + z_t - 2x^*(y_t, z_t)].
\end{aligned} \tag{19}$$

Summing (18) and (19), we conclude. \square

C Proof of Theorem 7

Before we move on to the proof of Theorem 7, we first provide a result from [67, 60] that quantifies the change in the function P over the iterations. We also provide its proof for the sake of completeness.

Lemma 13 (Lemma B.7 in [67]). *Suppose Assumptions 1, 2 and 3 hold. Consider the sm-AGDA iterate sequence $(x_t, y_t, z_t)_{t \in \mathbb{N}}$ for $p > \ell$, and let $Y^*(z) \triangleq \operatorname{argmax}_y \Psi(y; z)$ denote the set of maximizers of $\Psi(\cdot, z)$ for given z . For any $t \in \mathbb{N}$ and $y^*(z_{t+1}) \in Y^*(z_{t+1})$, it holds that*

$$P(z_{t+1}) - P(z_t) \leq \frac{p}{2} \langle z_{t+1} - z_t, z_{t+1} + z_t - 2x^*(y^*(z_{t+1}), z_t) \rangle.$$

Proof. Let $y^*(z_{t+1}) \in Y^*(z_{t+1})$ and $y^*(z_t) \in Y^*(z_t)$ be two arbitrary maximizers. We have

$$\begin{aligned}
P(z_{t+1}) - P(z_t) &= \min_x \max_y \hat{f}(x, y; z_{t+1}) - \min_x \max_y \hat{f}(x, y; z_t) \\
&= \max_y \min_x \hat{f}(x, y; z_{t+1}) - \max_y \min_x \hat{f}(x, y; z_t) \\
&= \Psi(y^*(z_{t+1}); z_{t+1}) - \Psi(y^*(z_t); z_t) \\
&\leq \Psi(y^*(z_{t+1}); z_{t+1}) - \Psi(y^*(z_{t+1}); z_t) \\
&= \hat{f}(x^*(y^*(z_{t+1}), z_{t+1}), y^*(z_{t+1}); z_{t+1}) - \hat{f}(x^*(y^*(z_{t+1}), z_t), y^*(z_{t+1}); z_t) \\
&\leq \hat{f}(x^*(y^*(z_{t+1}), z_t), y^*(z_{t+1}); z_{t+1}) - \hat{f}(x^*(y^*(z_{t+1}), z_t), y^*(z_{t+1}); z_t) \\
&= \frac{p}{2} (z_{t+1} - z_t)^\top [z_{t+1} + z_t - 2x^*(y^*(z_{t+1}), z_t)].
\end{aligned}$$

The first and the third equality above hold by the definition of $P(z)$ and $\Psi(y; z)$ functions; on the other hand, for the second equality, one needs strong duality to hold. This interchange is valid and can be justified by the simple fact that \hat{f} is strongly convex in x (therefore, it satisfies the PL condition in x), and it also satisfies the PL condition in y according to our assumption 2. It has been established in [61, Lemma 2.1] that the double-sided PL property allows one for the min-max switch. \square

Equipped with this lemma, the stage is set to prove Theorem 7 from Section 3. We first restate an extended version of this theorem, where the constants $\{c_i\}_{i=1}^8$ are provided explicitly.

Theorem 7. *Suppose Assumptions 1, 2, 3 and 4 hold. Consider the sm-AGDA algorithm with parameters $p > \ell$, $\beta \in (0, 1]$, $\tau_1 \in (0, \frac{1}{p+\ell}]$ and $\tau_2 > 0$ chosen such that*

$$c_0 \triangleq -\tau_2^2 \ell \nu + \tau_2 \left(1 - \frac{\ell}{2} \tau_2 - L_\Psi \tau_2 \right) \geq 0, \quad c'_0 \triangleq \frac{p}{3\beta} - \left(\frac{2p^2}{p-\ell} + 48\beta \frac{p^3}{(p-\ell)^2} \right) \geq 0$$

for some constant $\nu > 0$, where $L_\Psi = \ell \left(1 + \frac{p+\ell}{p-\ell} \right)$. Then,

$$\begin{aligned}
V_t - V_{t+1} &\geq c_1 \|\nabla_x \hat{f}(x_t, y_t; z_t)\|^2 + c_2 \|\nabla_y \hat{f}(x^*(y_t, z_t), y_t)\|^2 + c_3 \|x_t - z_t\|^2 \\
&\quad + c_4 \langle \nabla_x \hat{f}(x_t, y_t; z_t), \Delta_t^x \rangle + \langle c_5 \nabla_y \hat{f}(x_t, y_t) + c_6 \nabla_y \hat{f}(x^*(y_t, z_t), y_t), \Delta_t^y \rangle \\
&\quad + c_7 \|\Delta_t^x\|^2 + c_8 \|\Delta_t^y\|^2,
\end{aligned}$$

where the coefficients c_1 to c_8 have the following forms:

$$\begin{aligned}
c_1 &= \frac{\tau_1}{2} - 2 \left(\frac{1}{(p-\ell)^2} + \tau_1^2 \right) \left(c_0 \ell^2 + \frac{\ell}{\nu} + 48\beta p \left(\frac{p+\ell}{p-\ell} \right)^2 \ell^2 \tau_2^2 \right) - \left(c'_0 \beta^2 + \frac{\ell}{6} (1 + \ell \tau_2 + 2L_\Psi \tau_2) \right) \tau_1^2, \\
c_2 &= \frac{c_0}{2} - \frac{24\beta p}{(p-\ell)\mu} \left(1 + \tau_2 \frac{2p\ell}{p-\ell} \right)^2, \quad c_3 = c'_0 \beta^2 / 2,
\end{aligned}$$

$$\begin{aligned}
c_4 &= - \left(192\beta p \left(\frac{p+\ell}{p-\ell} \right)^2 \ell^2 \tau_2^2 + \frac{4\ell}{\nu} + 4c_0 \ell^2 + 2c'_0 \beta^2 \right) \tau_1^2 - \left((p+\ell)\tau_1 - 1 \right) \tau_1, \\
c_5 &= -\tau_2(1 + \ell\tau_2 + 2L_\Psi\tau_2), \quad c_6 = 2\tau_2, \\
c_7 &= - \left(96\beta p \left(\frac{p+\ell}{p-\ell} \right)^2 \ell^2 \tau_2^2 + \frac{2\ell}{\nu} + \frac{p+\ell}{2} + 2c_0 \ell^2 + \frac{\ell}{6}(1 + \ell\tau_2 + 2L_\Psi\tau_2) + c'_0 \beta^2 \right) \tau_1^2, \\
c_8 &= - \left(48\beta p \left(\frac{p+\ell}{p-\ell} \right)^2 + \frac{\ell}{2} + L_\Psi + 3\ell(1 + \ell\tau_2 + 2L_\Psi\tau_2) \right) \tau_2^2.
\end{aligned}$$

Furthermore, the **sm-AGDA** parameters can be chosen such that $c_1, c_2, c_3 > 0$.

Proof. Combining the inequalities in Lemmas 5, 6 and 13 gives us a lower bound of the form:

$$V_t - V_{t+1} \geq A_1 + A_2 + A_3 + A_4 + A_5 + A_6, \quad (20)$$

for any $y^*(z_{t+1}) \in Y^*(z_{t+1})$ appearing in A_3 , where

$$\begin{aligned}
A_1 &= \frac{\tau_1}{2} \|\nabla_x \hat{f}(x_t, y_t; z_t)\|^2 + \tau_2 \left(1 - \frac{\ell}{2} \tau_2 - L_\Psi \tau_2 \right) \|\nabla_y f(x_{t+1}, y_t)\|^2 + \frac{p}{2\beta} \|z_t - z_{t+1}\|^2, \\
A_2 &= 2\tau_2 \langle \nabla_y f(x^*(y_t, z_t), y_t) - \nabla_y f(x_{t+1}, y_t), \nabla_y f(x_{t+1}, y_t) \rangle, \\
A_3 &= 2p \langle z_{t+1} - z_t, x^*(y^*(z_{t+1}), z_t) - x^*(y_{t+1}, z_{t+1}) \rangle \\
A_4 &= -\tau_1((p+\ell)\tau_1 - 1) \langle \nabla_x \hat{f}(x_t, y_t; z_t), \Delta_t^x \rangle, \\
A_5 &= \langle 2\tau_2 \nabla_y f(x^*(y_t, z_t), y_t) - \tau_2(1 + \ell\tau_2 + 2L_\Psi\tau_2) \nabla_y f(x_{t+1}, y_t), \Delta_t^y \rangle, \\
A_6 &= -\frac{p+\ell}{2} \tau_1^2 \|\Delta_t^x\|^2 - \frac{\ell\tau_2^2}{2} \|\Delta_t^y\|^2 - L_\Psi \tau_2^2 \|\Delta_t^y\|^2.
\end{aligned}$$

Next, we provide lower bounds for several terms in the above inequality, including A_2 , A_3 , A_5 , $\|\nabla_y f(x_{t+1}, y_t)\|^2$ and $\|z_{t+1} - z_t\|^2$. At the end, using these bounds within (20), we will be able to establish a descent property for $\{V_t\}$, which will allow to apply our concentration result (Theorem 9) for deriving the desired high probability bounds.

Lower bound for A_2 . Using Cauchy-Schwarz inequality and ℓ -smoothness of f , we have

$$\begin{aligned}
A_2 &\geq -2\tau_2 \|\nabla_y f(x^*(y_t, z_t), y_t) - \nabla_y f(x_{t+1}, y_t)\| \|\nabla_y f(x_{t+1}, y_t)\| \\
&\geq -2\tau_2 \ell \|x_{t+1} - x^*(y_t, z_t)\| \|\nabla_y f(x_{t+1}, y_t)\| \\
&\geq -\tau_2^2 \ell \nu \|\nabla_y f(x_{t+1}, y_t)\|^2 - \ell \nu^{-1} \|x_{t+1} - x^*(y_t, z_t)\|^2, \quad \forall \nu > 0,
\end{aligned}$$

where last line follows from Young's inequality. Thus, by Lemma 18, we obtain for any $\nu > 0$

$$\begin{aligned}
A_2 &\geq -\tau_2^2 \ell \nu \|\nabla_y f(x_{t+1}, y_t)\|^2 - \frac{2\ell}{\nu} \left(1 + \frac{1}{\tau_1^2(p-\ell)^2} \right) \tau_1^2 \|\nabla_x \hat{f}(x_t, y_t; z_t)\|^2 \\
&\quad - \frac{4\ell}{\nu} \tau_1^2 \langle \nabla_x \hat{f}(x_t, y_t; z_t), \Delta_t^x \rangle - \frac{2\ell}{\nu} \tau_1^2 \|\Delta_t^x\|^2.
\end{aligned} \quad (21)$$

Lower bound for A_3 . By Cauchy-Schwarz inequality and Lemma 19,

$$\begin{aligned}
A_3 &= 2p \langle z_{t+1} - z_t, x^*(y^*(z_{t+1}), z_t) - x^*(y^*(z_{t+1}), z_{t+1}) \rangle \\
&\quad + 2p \langle z_{t+1} - z_t, x^*(y^*(z_{t+1}), z_{t+1}) - x^*(y_{t+1}, z_{t+1}) \rangle \\
&\geq -2p \|z_{t+1} - z_t\| \|x^*(y^*(z_{t+1}), z_t) - x^*(y^*(z_{t+1}), z_{t+1})\| \\
&\quad + 2p \langle z_{t+1} - z_t, x^*(y^*(z_{t+1}), z_{t+1}) - x^*(y_{t+1}, z_{t+1}) \rangle \\
&\geq -\frac{2p^2}{p-\ell} \|z_{t+1} - z_t\|^2 + 2p \langle z_{t+1} - z_t, x^*(y^*(z_{t+1}), z_{t+1}) - x^*(y_{t+1}, z_{t+1}) \rangle.
\end{aligned}$$

Hence, using Young's inequality, for all $\beta > 0$, we obtain

$$A_3 \geq - \left(\frac{p}{6\beta} + \frac{2p^2}{p-\ell} \right) \|z_{t+1} - z_t\|^2 - 6\beta p \|x^*(y^*(z_{t+1}), z_{t+1}) - x^*(y_{t+1}, z_{t+1})\|^2. \quad (22)$$

We now lower bound the second term on the right-hand side of (22). First, note that we have $x^*(y^*(z_{t+1}), z_{t+1}) = x^*(z_{t+1})$, which follows from the fact that $\min_x \max_y \hat{f}(x, y; z) = \max_y \min_x \hat{f}(x, y; z)$ for all z since \hat{f} is strongly convex in x and satisfies the PL condition in Assumption 2. Hence, using the inequality $\left\| \sum_{i=1}^N w_i \right\|^2 \leq N \sum_{i=1}^N \|w_i\|^2$, which holds for any $\{w_i\} \in \mathbb{R}^{d_1}$ and $N \geq 1$, we get

$$\|x^*(y^*(z_{t+1}), z_{t+1}) - x^*(y_{t+1}, z_{t+1})\|^2$$

$$\begin{aligned}
&\leq 4\|x^*(z_{t+1}) - x^*(z_t)\|^2 + 4\|x^*(z_t) - x^*(y_t^+(z_t), z_t)\|^2 \\
&\quad + 4\|x^*(y_t^+(z_t), z_t) - x^*(y_{t+1}, z_t)\|^2 + 4\|x^*(y_{t+1}, z_t) - x^*(y_{t+1}, z_{t+1})\|^2.
\end{aligned}$$

By Lemma 19 and Lemma 21, we observe that

$$4\|x^*(z_{t+1}) - x^*(z_t)\|^2 + 4\|x^*(y_{t+1}, z_t) - x^*(y_{t+1}, z_{t+1})\|^2 \leq \frac{8p^2}{(p-\ell)^2} \|z_{t+1} - z_t\|^2.$$

Using Lemma 22, we also have

$$4\|x^*(z_t) - x^*(y_t^+(z_t), z_t)\|^2 \leq \frac{4}{(p-\ell)\mu} \left(1 + \tau_2 \frac{2p\ell}{p-\ell}\right)^2 \|\nabla_y f(x^*(y_t, z_t), y_t)\|^2.$$

Finally, using Lemma 16, we get

$$\begin{aligned}
&4\|x^*(y_t^+(z_t), z_t) - x^*(y_{t+1}, z_t)\|^2 \\
&\leq 4\left(\frac{p+\ell}{p-\ell}\right)^2 \|y_t^+(z_t) - y_{t+1}\|^2 \\
&= 4\left(\frac{p+\ell}{p-\ell}\right)^2 \tau_2^2 \|\nabla_y f(x^*(y_t, z_t), y_t) - G_y(x_{t+1}, y_t, \xi_{t+1}^y)\|^2 \\
&= 4\left(\frac{p+\ell}{p-\ell}\right)^2 \tau_2^2 \|\nabla_y f(x^*(y_t, z_t), y_t) - (\nabla_y f(x_{t+1}, y_t) + \Delta_t^y)\|^2, \\
&\leq 4\left(\frac{p+\ell}{p-\ell}\right)^2 \tau_2^2 (2\ell^2 \|x^*(y_t, z_t) - x_{t+1}\|^2 + 2\|\Delta_t^y\|^2),
\end{aligned}$$

where the last inequality stems from the ℓ -smoothness of f . In view of Lemma 18, we may further upper bound the above quantity as follows:

$$\begin{aligned}
&4\|x^*(y_t^+(z_t), z_t) - x^*(y_{t+1}, z_t)\|^2 \\
&\leq 16\left(\frac{p+\ell}{p-\ell}\right)^2 \ell^2 \tau_1^2 \tau_2^2 \left[\left(\frac{1}{\tau_1^2(p-\ell)^2} + 1\right) \|\nabla_x \hat{f}(x_t, y_t; z_t)\|^2 + 2\langle \nabla_x \hat{f}(x_t, y_t; z_t), \Delta_t^x \rangle + \|\Delta_t^x\|^2 \right] \\
&\quad + 8\left(\frac{p+\ell}{p-\ell}\right)^2 \tau_2^2 \|\Delta_t^y\|^2.
\end{aligned}$$

Summing up the three intermediate inequalities we established above, we obtain

$$\begin{aligned}
&\|x^*(y^*(z_{t+1}), z_{t+1}) - x^*(y_{t+1}, z_{t+1})\|^2 \\
&\leq \frac{8p^2}{(p-\ell)^2} \|z_{t+1} - z_t\|^2 + \frac{4}{(p-\ell)\mu} \left(1 + \tau_2 \ell + \frac{\tau_2 \ell (p+\ell)}{p-\ell}\right)^2 \|\nabla_y f(x^*(y_t, z_t), y_t)\|^2 \\
&\quad + 16\left(\frac{p+\ell}{p-\ell}\right)^2 \ell^2 \left(\frac{1}{\tau_1^2(p-\ell)^2} + 1\right) \tau_1^2 \tau_2^2 \|\nabla_x \hat{f}(x_t, y_t; z_t)\|^2 \\
&\quad + 32\left(\frac{p+\ell}{p-\ell}\right)^2 \ell^2 \tau_1^2 \tau_2^2 \langle \nabla_x \hat{f}(x_t, y_t; z_t), \Delta_t^x \rangle \\
&\quad + 16\left(\frac{p+\ell}{p-\ell}\right)^2 \ell^2 \tau_1^2 \tau_2^2 \|\Delta_t^x\|^2 + 8\left(\frac{p+\ell}{p-\ell}\right)^2 \tau_2^2 \|\Delta_t^y\|^2.
\end{aligned}$$

In conclusion for A_3 , using (22) and the above inequality, we obtain after some rearrangement

$$\begin{aligned}
A_3 &\geq - \left(\frac{p}{6\beta} + \frac{2p^2}{p-\ell} + 48\beta \frac{p^3}{(p-\ell)^2} \right) \|z_{t+1} - z_t\|^2 - \left(96\beta p \left(\frac{p+\ell}{p-\ell}\right)^2 \ell^2 \tau_1^2 \tau_2^2 \right) \|\Delta_t^x\|^2 \\
&\quad - \left(\frac{24\beta p}{(p-\ell)\mu} \left(1 + \tau_2 \frac{2p\ell}{p-\ell}\right)^2 \right) \|\nabla_y f(x^*(y_t, z_t), y_t)\|^2 \\
&\quad - \left[96\beta p \left(\frac{p+\ell}{p-\ell}\right)^2 \ell^2 \left(\frac{1}{\tau_1^2(p-\ell)^2} + 1\right) \tau_1^2 \tau_2^2 \right] \|\nabla_x \hat{f}(x_t, y_t; z_t)\|^2 \\
&\quad - \left(192\beta p \left(\frac{p+\ell}{p-\ell}\right)^2 \ell^2 \tau_1^2 \tau_2^2 \right) \langle \nabla_x \hat{f}(x_t, y_t; z_t), \Delta_t^x \rangle - \left(48\beta p \left(\frac{p+\ell}{p-\ell}\right)^2 \tau_2^2 \right) \|\Delta_t^y\|^2.
\end{aligned} \tag{23}$$

Lower bound for A_5 . Below we first bound $\langle \nabla_y f(x_{t+1}, y_t), \Delta_t^y \rangle$, i.e.,

$$\begin{aligned}
\langle \nabla_y f(x_{t+1}, y_t), \Delta_t^y \rangle &= \langle \nabla_y f(x_t, y_t), \Delta_t^y \rangle + \langle \nabla_y f(x_{t+1}, y_t) - \nabla_y f(x_t, y_t), \Delta_t^y \rangle \\
&\leq \langle \nabla_y f(x_t, y_t), \Delta_t^y \rangle + \frac{1}{12\tau_2\ell} \|\nabla_y f(x_{t+1}, y_t) - \nabla_y f(x_t, y_t)\|^2 + 3\tau_2\ell\|\Delta_t^y\|^2 \\
&\leq \langle \nabla_y f(x_t, y_t), \Delta_t^y \rangle + \frac{\ell\tau_1^2}{12\tau_2} \|\hat{G}_x(x_t, y_t, \xi_{t+1}^x; z_t)\|^2 + 3\tau_2\ell\|\Delta_t^y\|^2 \\
&\leq \langle \nabla_y f(x_t, y_t), \Delta_t^y \rangle + \frac{\ell\tau_1^2}{6\tau_2} \|\nabla_x \hat{f}(x_t, y_t; z_t)\|^2 + \frac{\ell\tau_1^2}{6\tau_2} \|\Delta_t^x\|^2 + 3\tau_2\ell\|\Delta_t^y\|^2,
\end{aligned}$$

where the first inequality follows from Young's inequality, the second inequality follows from $\nabla_y f$ being ℓ -smooth and the update rule $x_{t+1} = x_t - \tau_1 \hat{G}_x(x_t, y_t, \xi_{t+1}^x; z_t)$, and in the third inequality we use $\Delta_t^x = \hat{G}_x(x_t, y_t, \xi_{t+1}^x; z_t) - \nabla_x \hat{f}(x_t, y_t; z_t)$. Thus, since $-\tau_2(1 + \ell\tau_2 + 2L_\Psi\tau_2) < 0$, for any $\tau_2 > 0$, we obtain

$$\begin{aligned}
A_5 &\geq -\tau_2(1 + \ell\tau_2 + 2L_\Psi\tau_2) \left(\frac{\ell\tau_1^2}{6\tau_2} \|\nabla_x \hat{f}(x_t, y_t; z_t)\|^2 + \frac{\ell\tau_1^2}{6\tau_2} \|\Delta_t^x\|^2 + 3\tau_2\ell\|\Delta_t^y\|^2 \right) \\
&\quad + \langle 2\tau_2 \nabla_y f(x^*(y_t, z_t), y_t) - \tau_2(1 + \ell\tau_2 + 2L_\Psi\tau_2) \nabla_y f(x_t, y_t), \Delta_t^y \rangle.
\end{aligned} \tag{24}$$

Lower bound for $\|\nabla_y f(x_{t+1}, y_t)\|^2$. Using Lemma 18 we can lower bound $\|\nabla_y f(x_{t+1}, y_t)\|^2$ as follows:

$$\begin{aligned}
\|\nabla_y f(x_{t+1}, y_t)\|^2 &\geq \frac{1}{2} \|\nabla_y f(x^*(y_t, z_t), y_t)\|^2 - \|\nabla_y f(x_{t+1}, y_t) - \nabla_y f(x^*(y_t, z_t), y_t)\|^2 \\
&\geq \frac{1}{2} \|\nabla_y f(x^*(y_t, z_t), y_t)\|^2 - \ell^2 \|x_{t+1} - x^*(y_t, z_t)\|^2 \\
&\geq \frac{1}{2} \|\nabla_y f(x^*(y_t, z_t), y_t)\|^2 \\
&\quad - 2\ell^2 \tau_1^2 \left[\left(\frac{1}{\tau_1^2(p - \ell)^2} + 1 \right) \|\nabla_x \hat{f}(x_t, y_t; z_t)\|^2 + 2\langle \nabla_x \hat{f}(x_t, y_t; z_t), \Delta_t^x \rangle + \|\Delta_t^x\|^2 \right].
\end{aligned}$$

We observe that $\|\nabla_y f(x_{t+1}, y_t)\|^2$ appears in both A_1 and the lower bound given in (21) for A_2 ; hence, grouping the two terms together and using the definition of $c_0 \geq 0$, we get

$$\begin{aligned}
&\left(\tau_2 \left(1 - \frac{\ell}{2} \tau_2 - L_\Psi \tau_2 \right) - \tau_2^2 \ell \nu \right) \|\nabla_y f(x_{t+1}, y_t)\|^2 = c_0 \|\nabla_y f(x_{t+1}, y_t)\|^2 \\
&\geq \frac{c_0}{2} \|\nabla_y f(x^*(y_t, z_t), y_t)\|^2 - 2c_0\ell^2 \left(\frac{1}{(p - \ell)^2} + \tau_1^2 \right) \|\nabla_x \hat{f}(x_t, y_t; z_t)\|^2 \\
&\quad - 2c_0\ell^2 \tau_1^2 \left(2\langle \nabla_x \hat{f}(x_t, y_t; z_t), \Delta_t^x \rangle + \|\Delta_t^x\|^2 \right).
\end{aligned} \tag{25}$$

Lower bound for $\|z_{t+1} - z_t\|^2$. Since $z_{t+1} = z_t + \beta(x_{t+1} - z_t)$ for some $\beta > 0$, we observe that:

$$\begin{aligned}
\|z_{t+1} - z_t\|^2 &= \beta^2 \|x_{t+1} - z_t\|^2 \\
&= \beta^2 \|x_t - z_t - \tau_1 \hat{G}_x(x_t, y_t, \xi_{t+1}^x; z_t)\|^2 \\
&\geq \beta^2 \left(\frac{1}{2} \|x_t - z_t\|^2 - \tau_1^2 \|\hat{G}_x(x_t, y_t, \xi_{t+1}^x; z_t)\|^2 \right),
\end{aligned}$$

and since $\hat{G}_x(x_t, y_t, \xi_{t+1}^x; z_t) = \nabla_x \hat{f}(x_t, y_t; z_t) + \Delta_t^x$, we obtain

$$\|z_t - z_{t+1}\|^2 \geq \frac{\beta^2}{2} \|x_t - z_t\|^2 - \beta^2 \tau_1^2 \|\nabla_x \hat{f}(x_t, y_t; z_t)\|^2 - 2\beta^2 \tau_1^2 \langle \nabla_x \hat{f}(x_t, y_t; z_t), \Delta_t^x \rangle - \beta^2 \tau_1^2 \|\Delta_t^x\|^2.$$

Note that $\|z_{t+1} - z_t\|^2$ appears in both A_1 and the lower bound given in (23) for A_3 ; hence, grouping the two terms together and using the definition of $c'_0 \geq 0$ Using (26), we obtain

$$\begin{aligned}
&\left(\frac{p}{2\beta} - \frac{p}{6\beta} - \frac{2p^2}{p - \ell} - 48\beta \frac{p^3}{(p - \ell)^2} \right) \|z_{t+1} - z_t\|^2 = c'_0 \|z_{t+1} - z_t\|^2 \\
&\geq -c'_0 \beta^2 \tau_1^2 \|\nabla_x \hat{f}(x_t, y_t; z_t)\|^2 + c'_0 \frac{\beta^2}{2} \|x_t - z_t\|^2 - 2c'_0 \beta^2 \tau_1^2 \langle \nabla_x \hat{f}(x_t, y_t; z_t), \Delta_t^x \rangle - c'_0 \beta^2 \tau_1^2 \|\Delta_t^x\|^2.
\end{aligned}$$

We conclude by combining all these lower bounds, i.e., the claimed Lyapunov descent inequality follows directly from summing (20), (21), (23), (24), (25) and (26). Finally, it follows after straightforward computations that there exist choice of sm-AGDA parameters which yield $c_1, c_2, c_3 > 0$ while satisfying the conditions $c_0 \geq 0$ and $c'_0 \geq 0$; in fact Corollary 8 provides such sm-AGDA parameters explicitly. This completes the proof. \square

D Proof of Corollary 8

The lower bound provided in Theorem 7 resembles the descent property we require for our concentration result in Theorem 9. To allow for its proper application, we develop a stepsize policy inspired by [63].

Corollary 8. *Under the premise of Theorem 7, consider the parameters $p = 2\ell$, $\tau_1 \in (0, \frac{1}{3\ell}]$, $\tau_2 = \frac{\tau_1}{48}$, $\beta = \alpha\mu\tau_2$ for any $\alpha \in (0, \frac{1}{406}]$. Then, $\frac{\tilde{A}_{t+1} - \tilde{A}_t}{\tau_1} \leq -\tilde{B}_t + \tilde{C}_{t+1} + \tilde{D}_{t+1}$ for all $t \in \mathbb{N}$, where $\nu = \frac{12}{\tau_1\ell}$ and*

$$\begin{aligned}\tilde{A}_t &\triangleq \tau_1 V_t, \quad \tilde{B}_t \triangleq \frac{\tau_1}{5} \|\nabla_x \hat{f}(x_t, y_t; z_t)\|^2 + \frac{\tau_2}{8} \|\nabla_y f(x^*(y_t, z_t), y_t)\|^2 + \frac{\beta p}{8} \|x_t - z_t\|^2 \\ \tilde{C}_{t+1} &\triangleq \left[\left(192\beta p \left(\frac{p+\ell}{p-\ell} \right)^2 \ell^2 \tau_2^2 + \frac{4\ell}{\nu} + 4c_0 \ell^2 + 2c'_0 \beta^2 \right) \tau_1^2 + \left((p+\ell)\tau_1 - 1 \right) \tau_1 \right] \langle \nabla_x \hat{f}(x_t, y_t; z_t), \Delta_t^x \rangle \\ &\quad + \tau_2 \langle (1 + \ell\tau_2 + 2L_\Psi\tau_2) \nabla_y f(x_t, y_t) - 2\nabla_y f(x^*(y_t, z_t), y_t), \Delta_t^y \rangle, \\ \tilde{D}_{t+1} &\triangleq 2\ell\tau_1^2 \|\Delta_t^x\|^2 + 8\ell\tau_2^2 \|\Delta_t^y\|^2.\end{aligned}$$

Proof. In view of Theorem 7, it suffices to prove that setting $p = 2\ell$, $\tau_1 \in (0, \frac{1}{3\ell}]$, $\tau_2 = \frac{\tau_1}{48}$, $\beta = \alpha\mu\tau_2$ for some positive $\alpha \leq \frac{1}{406}$ and $\nu = \frac{12}{\tau_1\ell}$ leads to both $c_0 \geq 0$ and $c'_0 \geq 0$; furthermore, we also need to show that this choice of parameters implies the following lower bounds:

$$(i) c_1 \geq \frac{\tau_1}{5}, \quad (ii) c_2 \geq \frac{\tau_2}{8}, \quad (iii) c_3 \geq \frac{p\beta}{8}, \quad (iv) c_7 \geq -2\ell\tau_1^2, \quad (v) c_8 \geq -8\ell\tau_2^2.$$

First, we show that our parameter choice implies that $c_0, c'_0 \geq 0$. Noting that $L_\Psi = 4\ell$, using $\tau_1 \leq \frac{1}{3\ell}$, we may bound c_0 from above and below as follows:

$$\begin{aligned}\tau_2 &\geq c_0 \triangleq -\tau_2^2 \ell \nu + \tau_2 \left(1 - \frac{\ell}{2} \tau_2 - L_\Psi \tau_2 \right) \\ &= \tau_2 \left(1 - \left(\frac{\ell}{2} + L_\Psi + \ell \nu \right) \frac{\tau_1}{48} \right) \geq \tau_2 \left(1 - \frac{9}{2 \cdot 144} - \frac{1}{4} \right) \geq \frac{1}{2} \tau_2 \geq 0.\end{aligned}\tag{26}$$

Moreover, since $\beta = \alpha\mu\tau_2$ and $\tau_2 \leq \frac{1}{144\ell}$, we get $\beta \leq \frac{\alpha}{144}$ using $\kappa \geq 1$. Hence, for $\alpha \leq \frac{1}{406}$,

$$0 \leq \frac{2p^2}{p-\ell} + 48\beta \frac{p^3}{(p-\ell)^2} = 8\ell(1 + 48\beta) = \left(\frac{\alpha}{36}(1 + \alpha/3) \right) \frac{p}{\beta} \leq \frac{p}{12\beta},\tag{27}$$

where the last inequality follows from $\alpha \leq \frac{1}{406} \leq \frac{3}{2}(\sqrt{5} - 1)$; therefore, $c'_0 \in [\frac{p}{4\beta}, \frac{p}{3\beta}]$.

Next, we prove bounds on c_1, c_2, c_3, c_7, c_8 separately.

Proof of part (i). Since $p = 2\ell$, $\nu = \frac{12}{\tau_1\ell}$ and $\tau_1 \leq \frac{1}{3\ell}$, we first observe that

$$\frac{2\ell}{\nu} \left(\frac{1}{(p-\ell)^2} + \tau_1^2 \right) = \frac{\tau_1}{6} (\tau_1^2 \ell^2 + 1) \leq \frac{\tau_1}{6} \left(\frac{1}{9} + 1 \right) = \frac{5}{27} \tau_1.\tag{28}$$

Furthermore, using $\tau_2 = \frac{\tau_1}{48}$, and $\beta = \alpha\mu\tau_2$, we obtain

$$\begin{aligned}96\beta p \left(\frac{p+\ell}{p-\ell} \right)^2 \ell^2 \tau_2^2 \left(\frac{1}{(p-\ell)^2} + \tau_1^2 \right) &= \left[96\beta \ell^2 p \frac{(p+\ell)^2}{(p-\ell)^4} \left(1 + \tau_1^2 (p-\ell)^2 \right) \frac{\tau_2^2}{\tau_1} \right] \tau_1 \\ &\leq \left[96 \cdot \alpha \tau_2 \mu \cdot 18\ell \left(1 + \frac{1}{9} \right) \frac{\tau_2^2}{\tau_1} \right] \tau_1 \\ &\leq 1920 \cdot \alpha \cdot \frac{\tau_2^3 \ell^2}{\tau_1} \cdot \frac{\mu}{\ell} \cdot \tau_1 \\ &\leq \frac{5\alpha}{2592} \tau_1,\end{aligned}\tag{29}$$

where last line follows from the fact that $\mu/\ell \leq 1$ and $\frac{\tau_2^3 \ell^2}{\tau_1} = \frac{\tau_1^2 \ell^2}{48^3} \leq \frac{1}{144^2 \cdot 48}$, in which we used $\tau_1 \leq \frac{1}{3\ell}$.

Since $\tau_2 \geq c_0 \geq 0$ and $-2\ell^2 \left(\frac{1}{(p-\ell)^2} + \tau_1^2 \right) \geq -\frac{20}{9}$, using $\tau_2 = \frac{\tau_1}{48}$, we obtain

$$-2c_0 \ell^2 \left(\frac{1}{(p-\ell)^2} + \tau_1^2 \right) \geq -\frac{20\tau_2}{9} = -\frac{5}{108} \tau_1.\tag{30}$$

Using $L_\Psi = 4\ell$, $\tau_1 \leq \frac{1}{3\ell}$ and $\tau_2 \leq \frac{1}{144\ell}$, we get

$$\frac{\ell}{6} (1 + \ell\tau_2 + 2L_\Psi\tau_2) \tau_1^2 \leq \frac{\ell}{6} \left(1 + \frac{1}{144} + \frac{8}{144} \right) \tau_1^2 \leq \frac{1}{18} \left(1 + \frac{1}{144} + \frac{8}{144} \right) \tau_1 = \frac{17}{288} \tau_1.\tag{31}$$

Using $\tau_1 \leq \frac{1}{3\ell}$, $\tau_2 \leq \frac{1}{144\ell}$, this implies

$$-c'_0\tau_1^2\beta^2 \geq -\frac{p}{3}\beta\tau_1^2 \geq -\frac{2\ell}{3} \cdot \frac{\alpha\mu}{144\ell} \frac{1}{3\ell}\tau_1 \geq -\frac{\alpha}{648}\tau_1. \quad (32)$$

Combining equations (28), (29), (30), (31) and (32), we obtain

$$\begin{aligned} c_1 &\geq \left(\frac{1}{2} - \frac{5}{27} - \frac{5\alpha}{2592} - \frac{5}{108} - \frac{17}{288} - \frac{\alpha}{648} \right) \tau_1 = \left(\frac{1}{2} - \frac{25}{108} - \frac{17+\alpha}{288} \right) \tau_1 \\ &= \frac{181-3\alpha}{864} \tau_1 \geq \frac{60-\alpha}{288} \geq \frac{\tau_1}{5}, \end{aligned} \quad (33)$$

for $\alpha \leq \frac{1}{406} < 2.4$, which completes the proof of part (i).

Proof of part (ii). Due to our parameter choice, we first note that

$$\frac{24\beta p}{(p-\ell)\mu} \left(1 + \tau_2 \frac{2p\ell}{p-\ell} \right)^2 = 48\alpha \left(1 + \tau_2 \frac{2p\ell}{p-\ell} \right)^2 \tau_2 \leq 96\alpha\tau_2 \leq \frac{\tau_2}{8}, \quad (34)$$

where last line follows from $\tau_2 \leq \frac{1}{144\ell}$ and $\alpha \leq \frac{1}{406}$. Finally, (26) implies that $\frac{c_0}{2} \geq \frac{\tau_2}{4}$; hence, $c_2 \geq (\frac{1}{4} - \frac{1}{8})\tau_2 = \frac{\tau_2}{8}$.

Proof of part (iii). We have shown that $c'_0 \geq \frac{p}{4\beta}$; hence, $c_3 \geq \frac{p\beta}{8}$.

Proof of part (iv). According to (26), $\tau_2 \geq c_0$; hence, we deduce that

$$-2c_0\ell^2 \geq -2\tau_2\ell^2 \geq -\frac{1}{72}\ell, \quad (35)$$

where the last inequality follows from $\tau_2 \leq \frac{1}{144\ell}$. Furthermore, we note that

$$-96\beta p \left(\frac{p+\ell}{p-\ell} \right)^2 \ell^2 \tau_2^2 = -1728\alpha\tau_2^3\ell^3\mu \geq -\frac{\alpha}{12^3}\ell, \quad (36)$$

with the last inequality following also from $\frac{\mu}{\ell} \leq 1$ and $\tau_2 \leq \frac{1}{144\ell}$. We also note that

$$-\frac{2\ell}{\nu} - \frac{p+\ell}{2} = -\left(\frac{\ell\tau_1}{6} + \frac{3}{2} \right) \ell \geq -\frac{14}{9}\ell.$$

Finally, since $c'_0 \leq \frac{p}{3\beta}$ according to (27), we get

$$-c'_0\beta^2 \geq -\beta^2 \frac{p}{3\beta} = -\frac{2}{3}\alpha\mu\tau_2\ell \geq -\frac{\alpha}{216}\ell, \quad (37)$$

where we used $\tau_2 \leq \frac{1}{144\ell}$. Thus, since $\alpha \in (0, 1)$, it follows from (35), (36), (37) and (31) that

$$c_7 \geq -\ell\tau_1^2 \left(\frac{1}{72} + \frac{\alpha}{12^3} + \frac{14}{9} + \frac{\alpha}{216} + \frac{17}{96} \right) \geq -2\ell\tau_1^2.$$

Proof of part (v). For c_8 , we may simply observe that

$$\begin{aligned} c_8 &= - \left(48\beta p \left(\frac{p+\ell}{p-\ell} \right)^2 + \frac{\ell}{2} + L_\Psi + 3\ell(1 + \ell\tau_2 + 2L_\Psi\tau_2) \right) \tau_2^2 \\ &= - \left(864\alpha\mu\tau_2 + \frac{1}{2} + 4 + 3(1 + \ell\tau_2 + 2L_\Psi\tau_2) \right) \ell\tau_2^2 \\ &\geq - \left(6\alpha\frac{\mu}{\ell} + \frac{1}{2} + 4 + 3 \left(1 + \frac{1}{144} + \frac{8}{144} \right) \right) \ell\tau_2^2 \geq -8\ell\tau_2^2, \end{aligned}$$

where we used $\mu/\ell \leq 1$, $L_\Psi = 4\ell$, $\tau_2 \leq \frac{1}{144\ell}$, and $\alpha < \frac{1}{20}$. \square

E Proof of Theorem 9

Theorem 9. Let $\{\mathcal{F}_t\}_{t \in \mathbb{N}}$ be a filtration on $(\Omega, \mathcal{F}, \mathbb{P})$. Let A_t, B_t, C_t, D_t be four stochastic processes adapted to the filtration such that there exist $\sigma_C, \sigma_D > 0$ and $\tau > 0$ such that for all $t \in \mathbb{N}$: (i) $B_t \geq 0$, (ii) $\mathbb{E}[e^{\lambda C_{t+1}} \mid \mathcal{F}_t] \leq e^{\lambda^2 \sigma_C^2 B_t}$ for all $\lambda > 0$, (iii) $\mathbb{E}[e^{\lambda D_{t+1}} \mid \mathcal{F}_t] \leq e^{\lambda \sigma_D^2}$ for all $\lambda \in [0, \frac{1}{\sigma_D^2}]$ and (iv) $\frac{A_{t+1} - A_t}{\tau} \leq -B_t + C_{t+1} + D_{t+1}$. Then, for any $\bar{q} \in (0, 1]$, we have

$$\mathbb{P} \left(\frac{\tau}{2} \sum_{t=0}^{T-1} B_t \leq (A_0 - A_T) + \tau\sigma_C^2 T + 2\tau \max\{2\sigma_C^2, \sigma_D^2\} \log \left(\frac{1}{\bar{q}} \right) \right) \geq 1 - \bar{q}.$$

Proof. For some fixed $\gamma > 0$, let

$$S_T \triangleq \gamma \sum_{t=0}^{T-1} B_t - (A_0 - A_T)$$

with the convention that $S_0 \triangleq 0$. For any $T \in \mathbb{N}$, we have

$$\begin{aligned} S_{T+1} &= \gamma \sum_{t=0}^T B_t - (A_0 - A_{T+1}) \\ &= \gamma \sum_{t=0}^{T-1} B_t - (A_0 - A_T) + \gamma B_T - (A_T - A_{T+1}) \\ &= S_T + \gamma B_T - (A_T - A_{T+1}) \\ &= S_T + (\gamma - \tau) B_T + \tau B_T - (A_T - A_{T+1}) \\ &\leq S_T + (\gamma - \tau) B_T + \tau C_{T+1} + \tau D_{T+1}, \end{aligned}$$

where the inequality follows from condition (iv) of the hypothesis. Hence, for any $0 < \lambda \leq \frac{1}{2\tau\sigma_D^2}$ and any $T \in \mathbb{N}$:

$$\begin{aligned} \mathbb{E}[e^{\lambda S_{T+1}} | \mathcal{F}_T] &\leq \mathbb{E}[e^{\lambda S_T} e^{\lambda(\gamma-\tau)B_T} e^{\lambda\tau C_{T+1}} e^{\lambda\tau D_{T+1}} | \mathcal{F}_T] \\ &\leq e^{\lambda S_T} e^{\lambda(\gamma-\tau)B_T} \mathbb{E}[e^{2\lambda\tau C_{T+1}} | \mathcal{F}_T]^{\frac{1}{2}} \mathbb{E}[e^{2\lambda\tau D_{T+1}} | \mathcal{F}_T]^{\frac{1}{2}} \\ &\leq e^{\lambda S_T} e^{\lambda(\gamma-\tau)B_T} \left(e^{4\lambda^2\tau^2\sigma_C^2 B_T} \right)^{\frac{1}{2}} \left(e^{2\lambda\tau\sigma_D^2} \right)^{\frac{1}{2}} \\ &= e^{\lambda S_T} e^{\lambda(\gamma-\tau+2\tau^2\lambda\sigma_C^2)B_T} e^{\lambda\tau\sigma_D^2}, \end{aligned}$$

where the first inequality follows from Cauchy-Schwarz and in the second one we use (ii) and (iii) of the hypothesis. Fixing $\gamma = \tau/2$ yields for all $0 < \lambda \leq \frac{1}{4\tau\sigma_C^2}$:

$$\gamma - \tau + 2\tau^2\lambda\sigma_C^2 = \tau \left(-\frac{1}{2} + 2\lambda\sigma_C^2\tau \right) \leq 0.$$

Therefore, for $0 < \lambda \leq \min \left\{ \frac{1}{4\tau\sigma_C^2}, \frac{1}{2\tau\sigma_D^2} \right\}$, using $B_T \geq 0$ by (i) of the hypothesis, we get

$$\mathbb{E}[e^{\lambda S_{T+1}} | \mathcal{F}_T] \leq e^{\lambda S_T} e^{\lambda\tau\sigma_D^2},$$

and rolling this recursion backwards and noting $S_0 = 0$ yields:

$$\mathbb{E}[e^{\lambda S_T}] \leq e^{\lambda\tau\sigma_D^2 T};$$

thus, using a Chernoff bound, we get

$$\mathbb{P}(S_T > t) \leq \mathbb{E}[e^{\lambda S_T}] e^{-\lambda t} \leq e^{\lambda(\tau\sigma_D^2 T - t)}.$$

Since for $\bar{q} \in (0, 1]$,

$$e^{\lambda(\tau\sigma_D^2 T - t)} \leq \bar{q} \iff t \geq \tau\sigma_D^2 T - \frac{1}{\lambda} \log(\bar{q}),$$

we have

$$\mathbb{P} \left(\frac{\tau}{2} \sum_{t=0}^{T-1} B_t \leq (A_0 - A_T) + \tau\sigma_D^2 T - \frac{1}{\lambda} \log(\bar{q}) \right) \geq 1 - \bar{q}.$$

The claim follows by taking $\lambda = \frac{1}{2\tau} \min \left\{ \frac{1}{2\sigma_C^2}, \frac{1}{\sigma_D^2} \right\}$. \square

F Proof of Theorem 10

Theorem 10. *In the premise of Corollary 8, **sm**-AGDA iterates (x_t, y_t) for $\tau_1 = \bar{\tau} \leq \frac{1}{3\ell}$ satisfy*

$$\mathbb{P} \left(\frac{1}{T} \sum_{t=0}^{T-1} [\|\nabla_x f(x_t, y_t)\|^2 + \kappa \|\nabla_y f(x_t, y_t)\|^2] \leq \mathcal{Q}_{\bar{q}, T}, \right) \geq 1 - \bar{q}, \quad \forall T \in \mathbb{N}, \quad \forall \bar{q} \in (0, 1],$$

for some $\mathcal{Q}_{\bar{q}, T} = \mathcal{O} \left(\frac{\kappa(\Delta_0 + b_0)}{\bar{\tau}T} + \kappa(\delta_x^2 + \delta_y^2) \left(\bar{\tau}\ell + \frac{1}{T} \log \left(\frac{1}{\bar{q}} \right) \right) \right)$ explicitly stated in Appendix F, where $\Delta_0 \triangleq \Phi(z_0) - \Phi^*$, $b_0 \triangleq 2 \sup_{x, y} \{\hat{f}(x_0, y; z_0) - \hat{f}(x, y_0; z_0)\}$.

As a first step, we provide a helper lemma that shows that our concentration result (Theorem 9) is applicable to the sm-AGDA -related processes $\tilde{A}_t, \tilde{B}_t, \tilde{C}_t, \tilde{D}_t$ introduced in Corollary 8.

Lemma 14. *Let $A_t = \tilde{A}_t, B_t = \tilde{B}_t, C_t = \tilde{C}_t, D_t = \tilde{D}_t$, where $\tilde{A}_t, \tilde{B}_t, \tilde{C}_t, \tilde{D}_t$ are defined in Corollary 8; moreover, let $\tau = \tau_1$, where $\tau_1 > 0$ is the primal stepsize in sm-AGDA . Then, the processes A_t, B_t, C_t, D_t are adapted to the filtration $\mathcal{F}_t \triangleq \mathcal{F}_t^y$, where \mathcal{F}_t^y is defined in (6), and they satisfy the conditions of Theorem 9 with the following constants:*

$$(i) \sigma_C^2 = \tau_1(240\delta_x^2 + 32\delta_y^2), \quad (ii) \quad \sigma_D^2 = 16\ell\tau_1^2\delta_x^2 + 64\ell\tau_2^2\delta_y^2.$$

Proof. The fact that A_t, B_t, C_t, D_t are measurable with respect to $\mathcal{F}_t = \mathcal{F}_t^y$ for any $t \in \mathbb{N}$ follows directly from the definition of \mathcal{F}_t . Note that x_t and y_t are also \mathcal{F}_t -measurable for all $t \in \mathbb{N}$. We prove part (i) and part (ii) separately.

Proof of part (i). First, recall that $C_{t+1} = \tilde{C}_{t+1} = -c_4 \langle \nabla_x \hat{f}(x_t, y_t; z_t), \Delta_t^x \rangle - \langle c_5 \nabla_y f(x_t, y_t) + c_6 \nabla_y f(x^*(y_t, z_t), y_t), \Delta_t^y \rangle$. We would like to show that $\mathbb{E}[e^{\lambda C_{t+1}} \mid \mathcal{F}_t] \leq e^{\lambda^2 \sigma_C^2 B_t}$ for all $\lambda > 0$. From Assumption 3, we note that for any $\lambda \geq 0$:

$$\mathbb{E} \left[\exp \left(\lambda \langle -c_4 \nabla_x \hat{f}(x_t, y_t; z_t), \Delta_t^x \rangle \right) \mid \mathcal{F}_t \right] \leq \exp \left(8\lambda^2 c_4^2 \|\nabla_x \hat{f}(x_t, y_t; z_t)\|^2 \delta_x^2 \right),$$

where we used [34, Lemma 3]. Now, given the value of c_4 in Theorem 7 and the convexity of $t \mapsto t^2$, we have

$$c_4^2 \leq 5 \left(192\beta p \left(\frac{p+\ell}{p-\ell} \right)^2 \ell^2 \tau_2^2 \tau_1^2 \right)^2 + 5\tau_1^2 \left((p+\ell)\tau_1 - 1 \right)^2 + 5 \left(\frac{4\ell}{\nu} \tau_1^2 \right)^2 + 5 \left(4c_0 \ell^2 \tau_1^2 \right)^2 + 5 \left(2c_0' \beta^2 \tau_1^2 \right)^2.$$

Now, leveraging the stepsize policy specified in Corollary 8, since $\alpha \in (0, 1)$, using (36) we get

$$5 \left(192\beta p \left(\frac{p+\ell}{p-\ell} \right)^2 \ell^2 \tau_2^2 \tau_1^2 \right)^2 \leq 20 \cdot \left(\frac{\alpha}{12^3} \ell \tau_1^2 \right)^2 \leq 20 \cdot \left(\frac{\alpha}{3 \cdot 12^3} \right)^2 \tau_1^2 \leq \frac{\tau_1^2}{4}.$$

Similarly, as $\tau_1 \leq \frac{1}{3\ell}$, have $|(p+\ell)\tau_1 - 1| \in [0, 1]$, which implies

$$5\tau_1^2 \left((p+\ell)\tau_1 - 1 \right)^2 \leq 5\tau_1^2.$$

Since $\nu = \frac{12}{\tau_1 \ell}$, we have $5 \left(\frac{4\ell}{\nu} \tau_1^2 \right)^2 \leq \frac{5}{9} \ell^4 \tau_1^6 \leq \frac{\tau_1^2}{4}$. Furthermore, using (26), we have $5 \left(4c_0 \ell^2 \tau_1^2 \right)^2 \leq 80\tau_1^4 \tau_2^2 \ell^4 \leq \frac{\tau_1^2}{4}$. Finally, (37) and $\alpha \in (0, 1)$ imply that

$$5 \left(2c_0' \beta^2 \tau_1^2 \right)^2 \leq 20 \left(\frac{\alpha}{216} \ell \tau_1 \right)^2 \tau_1^2 \leq \frac{\tau_1^2}{4}.$$

Thus, $c_4^2 \leq 6\tau_1^2$, which implies that

$$\mathbb{E} \left[\exp \left(-\lambda \langle c_4 \nabla_x \hat{f}(x_t, y_t; z_t), \Delta_t^x \rangle \right) \mid \mathcal{F}_t \right] \leq \exp \left(48\lambda^2 \tau_1^2 \|\nabla_x \hat{f}(x_t, y_t; z_t)\|^2 \delta_x^2 \right). \quad (38)$$

Moreover, noting Δ_t^y is revealed after Δ_t^x , using [34, Lemma 3] again along with the inequality $\|u + v\| \leq 2\|u\|^2 + 2\|v\|^2$, we have:

$$\mathbb{E} \left[\exp \left(-\lambda \langle c_5 \nabla_y f(x_t, y_t) + c_6 \nabla_y f(x^*(y_t, z_t), y_t), \Delta_t^y \rangle \mid \mathcal{F}_t, \Delta_t^x \right) \right] \quad (39)$$

$$= \mathbb{E} \left[\exp \left(\lambda \tau_2 \langle (1 + \ell\tau_2 + 2L_\Psi\tau_2) \nabla_y f(x_t, y_t) - 2\nabla_y f(x^*(y_t, z_t), y_t), \Delta_t^y \rangle \mid \mathcal{F}_t, \Delta_t^x \right) \right]$$

$$\leq \exp \left(8\lambda^2 \tau_2^2 \|(1 + \ell\tau_2 + 2L_\Psi\tau_2) \nabla_y f(x_t, y_t) - 2\nabla_y f(x^*(y_t, z_t), y_t)\|^2 \delta_y^2 \right)$$

$$\leq \exp \left(64\lambda^2 \tau_2^2 \|\nabla_y f(x^*(y_t, z_t), y_t)\|^2 \delta_y^2 + 16\lambda^2 \tau_2^2 (1 + \ell\tau_2 + 2L_\Psi\tau_2)^2 \|\nabla_y f(x_t, y_t)\|^2 \delta_y^2 \right)$$

$$\leq \exp \left(64\lambda^2 \tau_2^2 \left(\|\nabla_y f(x^*(y_t, z_t), y_t)\|^2 + \|\nabla_y f(x_t, y_t)\|^2 \right) \delta_y^2 \right), \quad (40)$$

where the last line follows from $0 < 1 + \ell\tau_2 + 2L_\Psi\tau_2 \leq 1 + \frac{1}{144} + \frac{8}{144} \leq 2$.

Thus, since Δ_t^y is revealed after Δ_t^x , using (38) and (40) together with the tower property of the conditional expectations, we get

$$\begin{aligned} & \mathbb{E} \left[\exp \left(-\lambda \left(c_4 \langle \nabla_x \hat{f}(x_t, y_t; z_t), \Delta_t^x \rangle + \langle c_5 \nabla_y f(x_t, y_t) + c_6 \nabla_y f(x^*(y_t, z_t), y_t), \Delta_t^y \rangle \right) \right) \right] \\ & \leq \exp \left(48\lambda^2 \tau_1^2 \|\nabla_x \hat{f}(x_t, y_t; z_t)\|^2 \delta_x^2 + 64\lambda^2 \tau_2^2 (\|\nabla_y f(x^*(y_t, z_t), y_t)\|^2 + \|\nabla_y f(x_t, y_t)\|^2) \delta_y^2 \right). \end{aligned} \quad (41)$$

Finally, observe that

$$\begin{aligned} \|\nabla_y f(x_t, y_t)\| - \|\nabla_y f(x^*(y_t, z_t), y_t)\| & \leq \|\nabla_y f(x_t, y_t) - \nabla_y f(x^*(y_t, z_t), y_t)\| \\ & \leq \ell \|x_t - x^*(y_t, z_t)\| \\ & \leq \frac{\ell}{p - \ell} \|\nabla_x \hat{f}(x_t, y_t; z_t)\|, \end{aligned}$$

where in the last inequality we used the $(p - \ell)$ -strong convexity of $\hat{f}(\cdot, y_t; z_t)$ and the fact that we have $\nabla \hat{f}_x(x^*(y_t, z_t), y_t; z_t) = 0$. Therefore, since $p = 2\ell$, we obtain

$$\|\nabla_y f(x_t, y_t)\|^2 \leq 2\|\nabla_y f(x^*(y_t, z_t), y_t)\|^2 + 2\|\nabla_x \hat{f}(x_t, y_t; z_t)\|^2. \quad (42)$$

Plugging this inequality into (41) yields

$$\begin{aligned} & \mathbb{E} \left[\exp \left(-\lambda \left(c_4 \langle \nabla_x \hat{f}(x_t, y_t; z_t), \Delta_t^x \rangle + \langle c_5 \nabla_y f(x_t, y_t) + c_6 \nabla_y f(x^*(y_t, z_t), y_t), \Delta_t^y \rangle \right) \right) \right] \\ & \leq \exp \left(\lambda^2 (48\tau_1^2 \delta_x^2 + 128\tau_2^2 \delta_y^2) \|\nabla_x \hat{f}(x_t, y_t; z_t)\|^2 + 192\lambda^2 \tau_2^2 \delta_y^2 \|\nabla_y f(x^*(y_t, z_t), y_t)\|^2 \right) \\ & \leq \exp \left(\lambda^2 \max \left\{ \frac{5}{\tau_1} (48\tau_1^2 \delta_x^2 + 128\tau_2^2 \delta_y^2), 1536\lambda^2 \tau_2 \delta_y^2 \right\} B_t \right) \\ & \leq \exp \left(\lambda^2 \tau_1 (240\delta_x^2 + 32\delta_y^2) B_t \right), \end{aligned}$$

where the last inequality follows from $\tau_2 = \frac{\tau_1}{48}$.

Proof of part (ii). Recall that $D_{t+1} \triangleq \tilde{D}_{t+1} = 2\ell\tau_1^2 \|\Delta_t^x\|^2 + 8\ell\tau_2^2 \|\Delta_t^y\|^2$. We would like to show that $\mathbb{E}[e^{\lambda D_{t+1}} \mid \mathcal{F}_t] \leq e^{\lambda \sigma_D^2}$ for all $\lambda \in [0, \frac{1}{\sigma_D^2}]$ for some $\sigma_D > 0$. First, observe that for any $\lambda > 0$ such that $\lambda \leq \min\{\frac{1}{16\ell\tau_1^2 \delta_x^2}, \frac{1}{64\ell\tau_2^2 \delta_y^2}\}$, we have

$$\begin{aligned} \mathbb{E}[e^{\lambda D_{t+1}} \mid \mathcal{F}_t] & = \mathbb{E} \left[e^{2\lambda\ell\tau_1^2 \|\Delta_t^x\|^2 + 8\lambda\ell\tau_2^2 \|\Delta_t^y\|^2} \right] \\ & \leq \mathbb{E} \left[e^{4\lambda\ell\tau_1^2 \|\Delta_t^x\|^2} \right]^{\frac{1}{2}} \mathbb{E} \left[e^{16\lambda\ell\tau_2^2 \|\Delta_t^y\|^2} \right]^{\frac{1}{2}} \\ & \leq \left(e^{32\lambda\ell\tau_1^2 \delta_x^2} \right)^{\frac{1}{2}} \left(e^{128\lambda\ell\tau_2^2 \delta_y^2} \right)^{\frac{1}{2}} \\ & \leq e^{\lambda(16\ell\tau_1^2 \delta_x^2 + 64\ell\tau_2^2 \delta_y^2)}, \end{aligned}$$

where we used [34, Lemma 2] in the second inequality. \square

Before completing the proof of Theorem 10, we provide another lemma that gives a lower bound on B_t in terms of the squared norm of the partial gradients, based on our choice of **sm**-AGDA parameters.

Lemma 15. *For any $t \in \mathbb{N}$, we have*

$$\|\nabla_x f(x_t, y_t)\|^2 + \kappa \|\nabla_y f(x_t, y_t)\|^2 \leq \max \left\{ \frac{20\kappa}{\tau_1}, \frac{16\kappa}{\tau_2}, \frac{32\ell}{\beta} \right\} B_t. \quad (43)$$

Proof. Since $\nabla_x \hat{f}(x_t, y_t; z_t) = \nabla_x f(x_t, y_t) + p(x_t - z_t)$, using $\|a + b\|^2 \leq 2\|a\|^2 + 2\|b\|^2$, we get

$$\|\nabla_x f(x_t, y_t)\|^2 \leq 2\|\nabla_x \hat{f}(x_t, y_t; z_t)\|^2 + 2p^2 \|x_t - z_t\|^2.$$

Hence, together with (42) and the definition of B_t , we obtain

$$\|\nabla_x f(x_t, y_t)\|^2 + \kappa \|\nabla_y f(x_t, y_t)\|^2$$

$$\begin{aligned}
&\leq (2+2\kappa)\|\nabla_x \hat{f}(x_t, y_t; z_t)\|^2 + 2\kappa\|\nabla_y f(x^*(y_t, z_t), y_t)\|^2 + 2p^2\|x_t - z_t\|^2 \\
&\leq \max\left\{\frac{(2+2\kappa)\cdot 5}{\tau_1}, \frac{2\kappa\cdot 8}{\tau_2}, \frac{2p^2\cdot 8}{\beta p}\right\} B_t \\
&\leq \max\left\{\frac{20\kappa}{\tau_1}, \frac{16\kappa}{\tau_2}, \frac{32\ell}{\beta}\right\} B_t.
\end{aligned}$$

with the last inequality following from $\kappa \geq 1$. \square

We may now provide our proof for Theorem 10.

Proof of Theorem 10. According to Lemma 14, the processes A_t, B_t, C_t , and D_t defined in the statement of Lemma 14 satisfy the conditions of Theorem 9 for $\tau = \tau_1$. Therefore, for any $\bar{q} \in [0, 1)$,

$$\mathbb{P}\left(\frac{\tau_1}{2} \sum_{t=0}^{T-1} B_t \leq \tau_1(V_0 - V_T) + \tau_1\sigma_D^2 T + 2\tau_1 \max\{2\sigma_C^2, \sigma_D^2\} \log\left(\frac{1}{\bar{q}}\right)\right) \geq 1 - \bar{q}.$$

Thus, dividing by $\frac{\tau_1}{2}T$ and using Lemma 15, we can conclude that with the probability at least $1 - \bar{q}$, the following event holds:

$$\begin{aligned}
&\frac{1}{T} \sum_{t=0}^{T-1} \|\nabla_x f(x_t, y_t)\|^2 + \kappa \|\nabla_y f(x_t, y_t)\|^2 \\
&\leq 2 \max\left\{\frac{20\kappa}{\tau_1}, \frac{16\kappa}{\tau_2}, \frac{32\ell}{\beta}\right\} \left(\frac{1}{T}(V_0 - V_T) + \sigma_D^2 + \frac{1}{T} \max\{4\sigma_C^2, 2\sigma_D^2\} \log\left(\frac{1}{\bar{q}}\right)\right). \tag{44}
\end{aligned}$$

Finally, we can relate the potential gap $V_0 - V_T$ to the primal suboptimality, i.e., Δ_0 , and to the duality gap, i.e., $b_0/2 = \sup_{x,y} \{\hat{f}(x_0, y; z_0) - \hat{f}(x, y_0; z_0)\}$, at the initialization, following the same arguments provided in [63]. More precisely, for $V(x, y, z) \triangleq \hat{f}(x, y; z) - 2\Psi(y, z) + 2P(z)$, we first observe that

$$\begin{aligned}
V_0 - V_T &\leq V_0 - \min_{x,y,z} V(x, y, z) = V_0 - \min_{x,y,z} \hat{f}(x, y; z) - 2\Psi(y, z) + 2P(z) \\
&\leq V_0 - \min_z P(z). \tag{45}
\end{aligned}$$

where last line follows from $\hat{f}(x, y; z) - \Psi(y, z) \geq 0$ for all y, z and $P(z) - \Psi(y, z) \geq 0$ for all y, z . Since $p = 2\ell$, we also note that

$$P(z_0) = \min_x \max_y f(x, y) + \ell\|x - z_0\|^2 \leq \max_y f(z_0, y) = \Phi(z_0).$$

Finally, since P is the Moreau envelope of Φ , we have $\min_z P(z) = \min_z \Phi(z)$; therefore,

$$\begin{aligned}
V_0 - \min_z P(z) &= \hat{f}(x_0, y_0; z_0) - 2\Psi(y_0, z_0) + 2P(z_0) - \min_z \Phi(z) \\
&\leq \Phi(z_0) - \min_z \Phi(z) + \hat{f}(x_0, y_0; z_0) - \Psi(y_0, z_0) + P(z_0) - \Psi(y_0, z_0) \\
&\leq \Phi(z_0) - \min_z \Phi(z) + \frac{1}{2}b_0 + \frac{1}{2}b_0 = \Delta_0 + b_0. \tag{46}
\end{aligned}$$

Note that $\tau_2 = \frac{\tau_1}{48}$ implies $16\kappa/\tau_2 \geq 20\kappa/\tau_1$, and $32\ell/\beta = \frac{32}{\alpha} \cdot \kappa/\tau_2 > 16\kappa/\tau_2$ since $\alpha \in (0, 1)$. Therefore,

$$2 \max\left\{\frac{20\kappa}{\tau_1}, \frac{16\kappa}{\tau_2}, \frac{32\ell}{\beta}\right\} = \frac{64}{\alpha} \cdot \kappa/\tau_2. \tag{47}$$

Therefore, combining (44), (45), (46) and (47), we conclude that $\mathcal{Q}_{\bar{q}, T}$ has the following explicit form:

$$\mathcal{Q}_{\bar{q}, T} = r_1 \left\{ \frac{\Delta_0 + b_0}{T} + r_2 + \frac{r_3}{T} \log\left(\frac{1}{\bar{q}}\right) \right\}, \tag{48}$$

where the constants r_1, r_2 and r_3 are defined as

$$r_1 = \frac{64}{\alpha} \frac{\kappa}{\tau_2}, \quad r_2 = \sigma_D^2 = 16\ell\tau_1 \left(\tau_1\delta_x^2 + \frac{1}{12}\tau_2\delta_y^2 \right), \quad r_3 = \max\{4\sigma_C^2, 2\sigma_D^2\} = 4\sigma_C^2 = 4\tau_1(240\delta_x^2 + 32\delta_y^2),$$

where the equalities follow from the expressions of σ_C^2 and σ_D^2 provided in Lemma 14. \square

G Proof of Corollary 12

Setting $\tau_1 = \bar{\tau}$ and $\tau_2 = \bar{\tau}/48$ for any $\bar{\tau} > 0$ implies that $\mathcal{Q}_{\bar{q},T}$ defined in (48) satisfies $\mathcal{Q}_{\bar{q},T} = \mathcal{O}\left(\frac{\kappa(\Delta_0+b)}{\bar{\tau}T} + \bar{\tau}\ell\kappa\delta^2 + \frac{\delta^2\kappa}{T}\log\left(\frac{1}{\bar{q}}\right)\right)$. Hence, setting $\bar{\tau} = \min\left(\frac{1}{3\ell}, \frac{48\sqrt{\Delta_0+b_0}}{\sqrt{T}\ell\delta^2}\right)$ ensures that

$$\mathcal{Q}_{\bar{q},T} = \mathcal{O}\left(\frac{(\Delta_0+b_0)\ell\kappa}{T} + \sqrt{\frac{(\Delta_0+b_0)\ell}{T}}\delta\kappa + \frac{\delta^2\kappa}{T}\log\left(\frac{1}{\bar{q}}\right)\right).$$

Finally, to obtain an $\mathcal{O}(\varepsilon, \varepsilon/\sqrt{\kappa})$ -stationary point, it suffices to have the above bound smaller than $\mathcal{O}(\varepsilon^2)$, which is guaranteed when the following three conditions are met up to a constant factor: (i) $\frac{(\Delta_0+b_0)\ell\kappa}{T} \leq \frac{\varepsilon^2}{3}$, (ii) $\sqrt{\frac{(\Delta_0+b_0)\ell}{T}}\delta\kappa \leq \frac{\varepsilon^2}{3}$, and (iii) $\frac{\delta^2\kappa}{T}\log\left(\frac{1}{\bar{q}}\right) \leq \frac{\varepsilon^2}{3}$. This is directly implied by the value $T_{\varepsilon, \bar{q}}$ given in our corollary statement.

H Supplementary Lemmas

In this section, we present a sequence of supplementary lemmas essential for deriving our main result, Theorem (10). Some of these results are well-known and are directly referenced. For others, we have improved specific algebraic constants. Additionally, some lemmas are extensions of existing bounds provided in expectation.

Lemma 16. *For any $z \in \mathbb{R}^{d_1}$ and $y_1, y_2 \in \mathbb{R}^{d_2}$, $\|x^*(y_1, z) - x^*(y_2, z)\| \leq \left(\frac{p+\ell}{p-\ell}\right)\|y_1 - y_2\|$.*

Proof. This result is provided in [63, Lemma C.1], which immediately follows from [39, Lemma B.2, part (c)]. \square

Lemma 17. *For any $z \in \mathbb{R}^{d_1}$, the map $y \mapsto \Psi(y, z) = \min_x \hat{f}(x, y, z)$ is $\ell\left(1 + \frac{p+\ell}{p-\ell}\right)$ -smooth.*

Proof. This result immediately follows from [39, Lemma B.2, part (d)]. Indeed, for any $y_1, y_2 \in \mathbb{R}^{d_2}$, we have

$$\begin{aligned} & \|\nabla_y \Psi(y_1, z) - \nabla_y \Psi(y_2, z)\| \\ &= \|\nabla_y f(x^*(y_1, z), y_1) - \nabla_y f(x^*(y_2, z), y_2)\| \\ &\leq \ell\|x^*(y_1, z) - x^*(y_2, z)\| + \ell\|y_1 - y_2\| \leq \left(1 + \frac{p+\ell}{p-\ell}\right)\ell\|y_1 - y_2\|, \end{aligned}$$

where the first equality follows from Danskin's theorem, the first inequality follows from ℓ -smoothness of f , and the last inequality follows from Lemma 16. \square

Lemma 18. *Consider the iterates (x_t, y_t, z_t) of the sm-AGDA algorithm. For any $t \in \mathbb{N}$,*

$$\begin{aligned} \|x_{t+1} - x^*(y_t, z_t)\|^2 &\leq 2\left(1 + \frac{1}{\tau_1^2(p-\ell)^2}\right)\tau_1^2\|\nabla_x \hat{f}(x_t, y_t; z_t)\|^2 \\ &\quad + 4\tau_1^2\langle \nabla_x \hat{f}(x_t, y_t; z_t), \Delta_t^x \rangle + 2\tau_1^2\|\Delta_t^x\|^2. \end{aligned}$$

Proof. For any $t \in \mathbb{N}$, using the fact that \hat{f} is strongly convex in x with modulus $(p-\ell)$ together with $x^*(y_t, z_t) = \operatorname{argmin}_x \hat{f}(x, y_t; z_t)$, and $x_{t+1} = x_t - \tau_1 \hat{G}_x(x_t, y_t, \xi_{t+1}^x; z_t)$, we get

$$\begin{aligned} \|x_{t+1} - x^*(y_t, z_t)\|^2 &\leq 2\|x_t - x^*(y_t, z_t)\|^2 + 2\|x_{t+1} - x_t\|^2 \\ &\leq \frac{2}{(p-\ell)^2}\|\nabla_x \hat{f}(x_t, y_t; z_t)\|^2 + 2\tau_1^2\|\hat{G}_x(x_t, y_t, \xi_{t+1}^x; z_t)\|^2. \end{aligned}$$

Using the identity $\hat{G}_x(x_t, y_t, \xi_{t+1}^x; z_t) = \Delta_t^x + \nabla_x \hat{f}(x_t, y_t; z_t)$ within the above inequality yields the desired result. \square

Lemma 19. *For any $y \in \mathbb{R}^{d_2}$, $z_1, z_2 \in \mathbb{R}^{d_1}$, we have:*

$$\|x^*(y, z_1) - x^*(y, z_2)\| \leq \frac{p}{p-\ell}\|z_1 - z_2\|.$$

Proof. This result follows from [67, Lemma B.2]. Indeed, since \hat{f} is strongly convex in x with modulus $p-\ell$, we get

$$\hat{f}(x^*(y, z_1), y; z_2) - \hat{f}(x^*(y, z_2), y; z_2) \geq \frac{p-\ell}{2}\|x^*(y, z_1) - x^*(y, z_2)\|^2. \quad (49)$$

Then swapping z_1, z_2 leads to

$$\hat{f}(x^*(y, z_2), y; z_1) - \hat{f}(x^*(y, z_1), y; z_1) \geq \frac{p - \ell}{2} \|x^*(y, z_1) - x^*(y, z_2)\|^2. \quad (50)$$

Furthermore, from the definition \hat{f} , it follows that

$$\begin{aligned} \hat{f}(x^*(y, z_2), y; z_1) - \hat{f}(x^*(y, z_2), y; z_2) &= \frac{p}{2} (\|x^*(y, z_2) - z_1\|^2 - \|x^*(y, z_2) - z_2\|^2) \\ &= \frac{p}{2} (\|z_1\|^2 - \|z_2\|^2 + 2\langle x^*(y, z_2), z_2 - z_1 \rangle); \end{aligned}$$

similarly, swapping z_1, z_2 in the above inequality leads to

$$\begin{aligned} \hat{f}(x^*(y, z_1), y; z_2) - \hat{f}(x^*(y, z_1), y; z_1) &= \frac{p}{2} (\|x^*(y, z_1) - z_2\|^2 - \|x^*(y, z_1) - z_1\|^2) \\ &= \frac{p}{2} (\|z_2\|^2 - \|z_1\|^2 - 2\langle x^*(y, z_1), z_2 - z_1 \rangle). \end{aligned}$$

Thus, summing the above two identities and applying Cauchy-Schwartz gives us

$$\begin{aligned} \hat{f}(x^*(y, z_2), y; z_1) - \hat{f}(x^*(y, z_2), y; z_2) + \hat{f}(x^*(y, z_1), y; z_2) - \hat{f}(x^*(y, z_1), y; z_1) \\ \leq p \|x^*(y, z_1) - x^*(y, z_2)\| \|z_1 - z_2\|. \end{aligned}$$

We can lower bound the left hand side of the above inequality using (49) and (50), which leads to

$$(p - \ell) \|x^*(y, z_1) - x^*(y, z_2)\|^2 \leq p \|x^*(y, z_1) - x^*(y, z_2)\| \|z_1 - z_2\|. \quad (51)$$

Rearranging this inequality yields the desired result. \square

Lemma 20. *For any $x \in \mathbb{R}^{d_1}$, $x \mapsto \Phi(x; z)$ is $(p - \ell)$ -strongly convex.*

Proof. For any $y \in \mathbb{R}^{d_2}, z \in \mathbb{R}^{d_1}$, $x \mapsto \hat{f}(x, y; z)$ is strongly convex with modulus $p - \ell$, i.e., $x \mapsto \hat{f}(x, y; z) - \frac{p - \ell}{2} \|x\|^2$ is convex. Then, $x \mapsto \sup_{y \in \mathbb{R}^{d_2}} \hat{f}(x, y; z) - \frac{p - \ell}{2} \|x\|^2$ is convex as it is the pointwise supremum of convex functions. Therefore, $x \mapsto \Phi(x; z) - \frac{p - \ell}{2} \|x\|^2$ is convex, and this implies $x \mapsto \Phi(x, z)$ is strongly convex with modulus $p - \ell$. \square

Lemma 21. *For all $z_1, z_2 \in \mathbb{R}^{d_1}$, we have*

$$\|x^*(z_1) - x^*(z_2)\| \leq \frac{p}{p - \ell} \|z_1 - z_2\|.$$

Proof. Using the result of Lemma 20, one can show this result following exactly the same arguments in the proof of Lemma 19. \square

Lemma 22. *For any $y \in \mathbb{R}^{d_2}, z \in \mathbb{R}^{d_1}$, it holds that*

$$\|x^*(z) - x^*(y^+(z), z)\|^2 \leq \frac{1}{(p - \ell)\mu} \left(1 + \tau_2 \ell \frac{2p}{p - \ell}\right)^2 \|\nabla_y f(x^*(y, z), y)\|^2.$$

Proof. The proof is the same as [63, Lemma C.2]. \square

I Further Details about Figure 2

In this section, we provide further details about how the empirical and theoretical quantiles are estimated in Figure 2 and are compared.

Generation of the theoretical quantiles $\mathcal{Q}_{q,T}$. For any given $q \in (0, 1)$, estimating an upper bound on $\mathcal{Q}_{q,T}$ requires estimating an upper bound on the quantity $\Delta_0 + b_0$ based on Theorem 10. Other constants such as r_1, r_2, r_3, ℓ , and μ are explicitly known in the setting of this experiment based on the NCPL game where $T = 10,000$ is fixed.

First, we set the initial point (x_0, y_0) randomly, where each component of x_0 and y_0 is sampled uniformly from the interval $[-20, 20]$, and we set $z_0 = x_0$. We then estimate an upper bound on the quantity $\Delta_0 + b_0$ numerically based on a grid search, resulting in $\Delta_0 + b_0 = 12$. Second, we generate a linear mesh I_m with a grid size $m = 0.0002$ over the interval $[0, 1]$. For $q \in I_m$, we calculate $\mathcal{Q}_{q,T}$ based on Theorem 10. Third, we generate a sequence of quantiles $\mathcal{Q}_{I_m,T}$. These quantiles are used to create a CDF via linear interpolation using the `scipy.interpolate` package's `interp1d` function in Python. Note that this quantile sequence generates a CDF over the values $\mathcal{Q}_{I_m,T}$.

Generation of the empirical quantiles of the random variable X_T . We generate 1,000 samples $\{X_T^{(i)}\}_{i=1}^{1000}$ from the sample paths corresponding to the NCPL game with $T = 10,000$, where $X_T = \frac{1}{T} \sum_{t=1}^T \|\nabla_x f(x_t, y_t)\|^2 + \kappa \|\nabla_y f(x_t, y_t)\|^2$ represents the path averages of the gradients. Quantiles for this sequence were generated over I_m using NumPy's quantile generator in Python, ensuring alignment with the mesh over which the theoretical quantiles were generated. Evidently, our theoretical quantiles dominate the empirical quantiles pointwise, demonstrating that in the challenging NCPL regime, our theory provides empirically verifiable guarantees on the tail behavior of the random variable X_T .

Comparison of quantiles. We plotted the CDF corresponding to the theoretical quantiles $\mathcal{Q}_{q,T}$ over the values of the empirical quantiles using a common mesh grid over the range of the empirical averages of the sample paths. In other words, we scaled the quantiles $\mathcal{Q}_{q,T}$ with an affine transformation so that their range matches the range of the empirical quantiles. This affine scaling preserves the shape of the distribution corresponding to the theoretical quantiles and allows for better visualization.